Complete suspension culture of human induced pluripotent stem cells supplemented with suppressors of spontaneous differentiation

Mami Matsuo-Takasaki[1], Sho Kambayashi[2], Yasuko Hemmi[1], Tamami Wakabayashi[1], Tomoya Shimizu[1], Yuri An[1], Kazuhiro Takeuchi[2], Masato Ibuki[2], Yoshikazu Kawai[2], Masafumi Umekage[3], Tomoaki M Kato[3], Michiya Noguchi[4], Koji Nakade[5], Yukio Nakamura[4], Tomoyuki Nakaishi[2], Masayoshi Tsukahara[3], Yohei Hayashi[1,6]*.

[1]iPS Cell Advanced Characterization and Development Team, RIKEN BioResource Research Center, Ibaraki, 305-0074, Japan; [2]Regenerative Medicine and Cell Therapy Laboratories, KANEKA CORPORATION, Kobe, 650-0047, Japan; [3]Research and Development Center, CiRA Foundation, Kyoto, 606-8507, Japan; [4]Cell Engineering Division, RIKEN BioResource Research Center, Ibaraki, 305-0074, Japan; [5]Gene Engineering Division, RIKEN BioResource Research Center, Ibaraki, 305-0074, Japan; [6]Faculty of Medicine, University of Tsukuba, Ibaraki, 305-8575, Japan.

*For corresponding:

yohei.hayashi@riken.jp (YHa)

Abstract

Human induced pluripotent stem cells (hiPSCs) are promising resources for producing various type of tissues in regenerative medicine; however, a scalable culture system that can precisely control the cell status for hiPSCs is not developed yet. Utilizing suspension culture without microcarriers or special materials allows for massive production, automation, cost effectiveness, and safety assurance in industrialized regenerative medicine. Here, we found that hiPSCs cultured in suspension conditions with continuous agitation without any microcarriers or extracellular matrix components were more prone to spontaneous differentiation than those cultured in conventional adherent conditions. Adding PKCβ and Wnt signaling pathway inhibitors in the suspension conditions suppressed the spontaneous differentiation of hiPSCs into ectoderm and mesendoderm, respectively. In these conditions, we successfully completed culture processes of hiPSCs including the generation of hiPSCs from peripheral blood mononuclear cells with the expansion of bulk population and single-cell sorted clones, long-term culture with robust self-renewal characteristics, single cell cloning, direct cryopreservation from suspension culture and their successful recovery, and efficient mass production of a clinical-grade hiPSC line. Our results demonstrate that precise control of hiPSC status in suspension culture conditions paves the way for their stable and automated clinical application.

Introduction

Human induced pluripotent stem cells (hiPSCs) are promising resources for various types of tissues in regenerative medicine (Takahashi *et al*, 2007; Yu *et al*, 2007). To enable cell therapy from hiPSCs, the development of a large-scale manufacturing system is essential because massive cell numbers are required to compose transplantable cells which are enough to rescue the desired physiological function (Chen *et al*, 2014; Kim & Kino-Oka, 2020; Tannenbaum & Reubinoff, 2022). In general, hiPSCs are believed to possess their scaffold dependency, thus are cultured under adhesion and monolayer culture conditions (Hayashi & Furue, 2016; Xu *et al*, 2001). However, utilizing suspension culture without microcarriers or special materials allows for massive production, automation, cost-effectiveness, and safety assurance in industrialized regenerative medicine.

Several attempts have been made to develop suspension culture technologies enabling rapid and large-scale preparation of hiPSCs (Amit *et al*, 2010; Amit *et al*, 2011; Dang *et al*, 2004; Elanzew *et al*, 2015; Horiguchi & Sakai, 2016; Hunt *et al*, 2014; Ibuki *et al*, 2019; Kehoe *et al*, 2010; Kim *et al*, 2019; Krawetz *et al*, 2010; Kwok *et al*, 2018; Lam *et al*, 2016; Nath *et al*, 2017; Oh *et al*, 2009; Olmer *et al*, 2012; Rohani *et al*, 2020; Shafa *et al*, 2012; Singh *et al*, 2010; Steiner *et al*, 2010; Wang *et al*, 2013; Zweigerdt *et al*, 2011) (Summarized in Table 1). These studies have achieved long-term culture and/or mass expansion of hiPSCs and/or human embryonic stem cells (hESCs) in suspension conditions. However, completed processes from clonal hiPSC generation to mass production of hiPSCs based on the precise control of cell status have not yet been achieved.

In this study, we have investigated what hampers the stable maintenance of undifferentiated cell states in suspension conditions. HiPSCs cultured in suspension conditions with continuous agitation without any microcarriers or extracellular matrix (ECM) components were more prone to spontaneous differentiation than those cultured in conventional adherent conditions. From screening of candidate molecules to suppress the spontaneous differentiation of hiPSCs, we have identified that inhibitors of PKCβ and Wnt signaling pathways suppress their differentiation into ectoderm and mesendoderm, respectively. In these conditions, we aimed to complete the processes of handling hiPSCs including the generation of hiPSCs with the expansion of bulk population and single-cell sorted clones, long-term culture with robust self-renewal characteristics, single-cell cloning, direct cryopreservation from suspension culture and their successful recovery, and efficient mass production of a clinical-grade hiPSC line.

Results

Suspension cultured hiPSCs are prone to spontaneous differentiation.

First, we investigated whether the quality of hiPSCs in suspension and adherent conditions are equivalent or not. HiPSCs cultured in a conventional medium with continuous agitation (90 rpm) in non-adhesive cell culture plates for 2 passages (5 days during passages) were examined (Figure 1A). In suspension culture on day 5 and 10, hiPSCs formed round cell assemblies with slightly uneven surfaces (Figure 1B). Gene expression analysis with RT-qPCR revealed that the expression of differentiation markers, such as PAX6 (ectoderm), SOX17 (endoderm), and T (mesoderm) increased in suspension-cultured hiPSCs for 10 days (Figure 1C). To monitor the spontaneous differentiation at single cell resolution, we established knock-in reporter hiPSC lines of PAX6-tdTomato and SOX17-tdTomato to visualize and quantify the expression of PAX6 and SOX17 at protein level, respectively (Figure 1—figure supplement 1A–H). tdTomato-positive cells were clearly observed in day 10 samples in suspension-cultured hiPSCs, whereas no positive cells were observed in adherent culture conditions (Figure. 1D). Flow cytometric analysis revealed that hiPSCs in suspension-culture conditions contained non-negligible percentages of PAX6-tdTomato-positive and SOX17-tdTomato-positive cells (Figure. 1E and 1F). Western blot analysis revealed that protein expression of PAX6 and SOX17 in suspension-culture was significantly increased (Figure 2—figure supplement 1A–D). The ratio of positive cells for a cell surface marker for undifferentiated hiPSCs, TRA1-60, was significantly lower in suspension-culture conditions (Figure 2—figure supplement 1E and F). These results suggest that a portion of hiPSCs was spontaneously differentiated in suspension conditions when cultured in conventional medium. To examine global changes in gene expression patterns between suspension and adherent conditions, whole-transcriptomic RNA-seq experiments with statistical tests were performed. Gene Set Enrichment Analysis (GSEA) of all the genes and Gene Ontology Enrichment Analysis (GOEA) on differentially-regulated genes revealed that, in suspension conditions, number of genes involved in differentiation toward various tissues and cell-cell adhesions were significantly up-regulated, whereas genes involved in nucleotide metabolism, hypoxic responses, and extracellular matrix organization were significantly-down-regulated (Figure 1G–J). These results suggest that hiPSCs in suspension conditions are in the process of spontaneous differentiation into various cell lineages and are characterized with specific signatures of gene expression patterns.

Wnt signaling inhibitors suppress spontaneous mesendodermal differentiation in suspension culture condition.

We next investigated the factors having an inhibitory effect on hiPSCs spontaneous differentiation in suspension conditions (Figure 2A). Since Wnt signaling induces the differentiation of human pluripotent stem cells into mesendoderm lineages (Nakanishi *et al*, 2009;

105 Sumi *et al*, 2008; Tran *et al*, 2009; Vijayaragavan *et al*, 2009; Woll *et al*, 2008), and is
106 endogenously involved in the regulation of mesendoderm differentiation of pluripotent stem cells
107 (Dziedzicka *et al*, 2021), we hypothesized that adding Wnt signaling inhibitors/activator may
108 alter spontaneous differentiation of hiPSCs into mesendoderm. Therefore, Wnt signaling
109 inhibitors, IWP2 or IWR-1-endo (Chen *et al*, 2009), or an activator, CHIR99021 (Ring *et al*,
110 2003), were added to the culture medium under suspension conditions. HiPSC aggregates treated
111 with and without inhibitors showed similar shapes (Figure 2B). In contrast, hiPSC aggregates
112 treated with CHIR99021 formed heterogeneously shaped cyst-like structures, suggesting that they
113 were largely differentiated. In samples treated with inhibitors, both T and SOX17 expression
114 levels were significantly reduced to the level of adherent-cultured hiPSCs; however, there was no
115 reduction in PAX6 expression (Figure 2C). In contrast, CHIR99021-treated cell aggregates
116 showed markedly decreased OCT4 and increased T and SOX17 expression. Additionally, SOX17
117 protein expression was suppressed in hiPSCs treated with IWR-1-endo in suspension-culture
118 conditions, although its expression increased in hiPSCs in suspension conditions with
119 conventional culture medium compared to adherent conditions (Figure 2—figure supplement 1A
120 and B). These results indicate that Wnt signaling inhibitors effectively suppressed
121 mesendodermal differentiation in suspension-culture, but was insufficient to suppress ectodermal
122 differentiation.

123 **PKC signal inhibitors suppress spontaneous neuroectododermal differentiation in**
124 **suspension conditions.**
125 To identify molecules with inhibitory activity on neuroectodermal differentiation, hiPSCs were
126 treated with candidate molecules in suspension conditions. Out of the candidate molecules tested
127 (listed in Supplementary Table 1), Go6983, a pan-PKC inhibitor (Gschwendt *et al*, 1996), showed
128 the strongest inhibition against PAX6 expression (Figure 2D). Further, simultaneous treatment
129 with Go6983 and IWR-1-endo decreased PAX6, T, and SOX17 expression, while maintaining
130 OCT4 expression. To confirm these screening test results, the dose dependent effect of Go6983 or
131 another PKCα, β, γ inhibitor GF109203X (GFX) (Toullec *et al*, 1991) on the inhibition of
132 PAX6 expression was observed at constant concentration of IWR-1-endo (Figure 2E and F).
133 These results demonstrated that the inhibition of PKC signaling pathway effectively suppress
134 neuroectoderm differentiation in hiPSCs cultured in suspension conditions. Furthermore, we
135 tested various PKC inhibitors to suppress neuroectodermal differentiation from hiPSCs in
136 suspension culture using the 201B7 hiPSC line (Figure 2—figure supplement 2A). The
137 suppression of PAX6 expression in hiPSCs cultured in suspension conditions was observed with
138 PKC inhibitors, enzastaurin (Ly317615), sotrastaurin (AEB071), Ro-32-0432, Go6983,
139 GF109203X, and LY333531, which possessed PKCβ inhibition activity (Figure 2—figure
140 supplement 2B-D); however, sotrastaurin and Ro-32-0432 also showed growth inhibition. Thus,
141 for the rest of the study, a PKCβ specific inhibitor, LY333531 (Jirousek *et al*, 1996) was used. As
142 compared to controls, another hiPSC line, WTc11, cultured in suspension conditions treated with

143 IWR-1-endo and LY333531 formed homogenous, round, smooth-surfaced aggregates (Figure.
144 3A). PAX6 expression was strongly suppressed by the addition of LY333531 (Figure. 3B).
145 Furthermore, after adding IWR-1-endo, the inhibitory effect of PAX6 expression was further
146 enhanced, and simultaneously, OCT4 expression was restored to the same level as in the
147 adherent-culture. PAX6 protein expression was also suppressed in hiPSCs treated with IWR-1-
148 endo and LY333531 in suspension-culture conditions while its expression increased in
149 suspension conditions with conventional culture medium compared to adherent-conditions
150 (Figure 2—figure supplement 1C and D). The ratio of TRA-1-60-positive cells was higher in
151 suspension-culture conditions supplemented with IWR-1-endo and LY333531 than in control
152 conditions without these inhibitors (Figure 2—figure supplement 1E and F). These results
153 indicate that the maintenance of suspension-cultured hiPSCs is specifically facilitated by the
154 combination of PKCβ and Wnt signaling inhibition.

155 We examined the effect of PKCβ and Wnt inhibitors on global gene expression of hiPSCs under
156 suspension conditions. RNA-seq data were obtained from suspension conditions in absence of
157 inhibitors (Sus), supplemented with IWR-1-endo (IWR), LY333531 (LY), IWR-1-endo and
158 LY333531 (IWRLY), and adherent conditions (Ad). Hierarchical clustering obtained from these
159 data showed that LY and IWRLY were grouped closely with Ad (Figure 3C). In contrast, Sus and
160 IWR were both grouped as discrete populations from Ad. Additionally, hierarchical clustering in
161 gene expression among these conditions was supported by principal component 1 (PC1) in the
162 principal component analysis (PCA) (Figure 3D). In contrast, PC2 represented genes related to
163 the effects of specific inhibitors under these conditions. Next, we investigated the effect of
164 LY333531 and IWR-1-endo in suspension culture. Many genes involved in pluripotency: KLF4
165 and ID1, and epithelial cell-cell interactions: CDH1 (E-cadherin), were significantly up-regulated
166 in IWRLY, while many transcription factors involved in differentiation: PAX2, 3, 5, and 8, SP5,
167 DBX1, and TFAP2B, were down-regulated in IWRLY (Figure 3E). GSEA and GOEA on down-
168 regulated genes in IWRLY showed that the expression of developmentally associated genes,
169 whose expression was elevated in Sus, was generally reduced in IWRLY (Figure 3F and G).
170 GOEA on up-regulated genes revealed gene sets involved in epithelial cell types (Figure 3H). As
171 compared to Ad, genes involved in sensory system development, cell-cell adhesion, and Wnt and
172 PI3K signaling pathways were up-regulated in IWRLY, and genes involved in nucleotide
173 metabolism and hypoxic responses were down-regulated under IWRLY conditions (Figure 3—
174 figure supplement 1A-D). These results suggest that PKCβ and Wnt signaling inhibitors in
175 suspension conditions regulate global gene expression patterns to suppress spontaneous
176 differentiation, albeit remaining expression signatures of suspension culture, possibly due to the
177 microenvironment within the formed aggregates and physiological differences.

178 Further, we examined the expression pattern changes in specific isoforms of PKCs in hiPSCs
179 cultured in adherent/suspension conditions. RNA expression of PKCα (PRKCA) and PKCβ
180 (PRKCB) was significantly up-regulated under suspension-culture conditions compared to

181 adhesion conditions (Figure 3—figure supplement 2A). Moreover, phospho-PKCβ protein
182 expression was significantly elevated (Figure 3—figure supplement 2B and C). These results
183 suggest that elevated expression of PKCβ in suspension-cultured hiPSCs could affect the
184 spontaneous differentiation.

185 **Simultaneous inhibition of PKCβ and Wnt signals maintains undifferentiated hiPSCs in**
186 **suspension for long-term culture.**
187 We next performed long-term culture for 10 passages in suspension conditions and compared
188 hiPSC growth in presence of LY333531 or Go6983. When hiPSCs were seeded at 4×10^5
189 cells/well, the average cell number reached approximately 12-fold after 5 days under both
190 conditions (Figure 4A and B). After 10 passages, aggregates of hiPSCs cultured in the presence
191 of LY333531 showed a uniform spherical shape, whereas aggregates cultured in the presence of
192 Go6983 were heterogeneously spherical (Figure 4C). Notably, in LY333531-treated cells, OCT4-
193 positive cell numbers were significantly higher than in Go6983-treated samples, as determined by
194 immunostaining (Figure 4D and E). To evaluate whether hiPSCs cultured in suspension
195 conditions with PKCβ and Wnt signaling inhibitors for 10 passages maintain pluripotency, we
196 performed embryoid body (EB) formation assay. These EBs contained positive cells for TUJ1,
197 SMA, and AFP as ectodermal, mesodermal, and endodermal marker, respectively (Figure 4F).
198 Comparative genomic hybridization (CGH) array analysis showed that hiPSCs cultured long-term
199 in the presence of PKCβ and Wnt inhibitors retained their normal human karyotype (Figure 4G).
200 These results indicate that, for long-term culture, inhibition of Wnt signaling and PKCβ in
201 suspension conditions was sufficient to maintain the self-renewal, pluripotency, and genomic
202 integrity of hiPSCs.

203 We further investigated whether the effects of PKCβ and Wnt inhibitors on suppressing hiPSCs
204 spontaneous differentiation in suspension-culture conditions are applicable to other culture
205 medium. Morphologies and gene expression profile of hiPSCs, cultured in suspension conditions
206 with another commercially available maintenance medium, StemScale (ThermoFisher Scientific,
207 Inc., MA, USA), were examined (Figure 4—figure supplement 1A). HiPSCs cultured in
208 suspension treated with IWR-1-endo and LY333531 formed homogenously round and smooth-
209 surfaced aggregates compared to controls (Figure 4—figure supplement 1B). The differentiation
210 markers expression, which was elevated under suspension conditions, was suppressed by the
211 simultaneous addition of PKCβ and Wnt signal inhibitors, as observed with StemFit medium
212 (Figure 4—figure supplement 1C and D). These results suggest that conventional suspension
213 culture methods might contain spontaneous differentiating cells and that the addition of inhibitors
214 of PKCβ and Wnt signaling pathways to culture medium generally suppresses spontaneous
215 differentiation.

216 **Mass and clonal expansion of hiPSCs in suspension conditions supplemented with inhibitors**
217 **of PKCβ and Wnt signaling pathways.**

218 For the clinical applications of hiPSCs, its homogenous mass production is required to obtain
219 sufficient quantities. To test the feasibility of mass production under suspension-culture
220 conditions supplemented with PKCβ and Wnt signal inhibitors, we first performed suspension-
221 culture using healthy-donor derived hiPSC lines, 1383D6 and 1231A3, in a 30 mL bioreactor
222 with stirring blade and demonstrated that undifferentiated hiPSCs were efficiently maintained in
223 this condition (Figure 5—figure supplement 1A). These cell lines showed higher cell density in
224 the bioreactor at each passage after 3 days (Figure 5—figure supplement 1B). Under these
225 conditions, the concentration of glucose decreased daily (Figure 5—figure supplement 1C),
226 whereas that of L-lactic acid increased (Figure 5—figure supplement 1D). These results indicate
227 that the cell lines proliferated with active energy consumption. Further, RT-qPCR analysis
228 showed no marked differences in the undifferentiated and differentiation markers expression
229 between hiPSCs cultured in adhesion vs. suspension with PKCβ and Wnt inhibitors (Figure 5—
230 figure supplement 1E and F). Flow cytometric analysis showed that more than 90% of these cells
231 were positive for pluripotency marker proteins: NANOG, OCT4, and SOX2 (Figure 5—figure
232 supplement 1G). G-band analysis of suspension-cultured hiPSCs after five passages revealed
233 normal karyotype (Figure 5—figure supplement 1H). These results demonstrate that
234 undifferentiated hiPSCs were efficiently maintained in the bioreactor using the culture medium
235 supplemented with inhibitors of PKCβ and Wnt signaling pathways.

236 Next, we expanded hiPSCs in a large-scale culture system under perfusion conditions in the
237 presence of IWR-1-endo and LY333531. In this experiment, clinical-grade hiPSC line, Ff-l14s04,
238 which is derived from PBMCs of a donor carrying homozygous alleles for major HLA loci
239 (HLA-A, HLA-B, and HLA-DR) was used (Kitano *et al*, 2022). Large-scale hiPSCs preparation
240 using a perfusion-culture system with 320 mL bioreactor having stirred-wing was performed in
241 GMP-compliant, clinical grade StemFit AK03N medium containing IWR-1-endo and LY333531
242 (Figure 5A). When the culture was started at 1×10^5 cells/mL in 320 mL medium, hiPSCs
243 proliferated nearly 10-fold after 3 to 4 days and reached approximately 1×10^9 cells in total to
244 produce ~300 stock vials (1×10^6 cells/vial). This large-scale culture was repeated three times
245 (Passages 1, 2, and 3), and hiPSCs obtained at each passage were characterized. These samples
246 showed similar or higher viability (>90%) to that of adherent-culture derived cells (Figure 5B).
247 When compared to adherent conditions, these samples in suspension-culture showed a similar or
248 higher proliferation rate (Figure 5C). Cells obtained from large-suspension cultures formed
249 typical hiPSC-like colonies, after vials were thawed and seeded in adherent-culture conditions
250 (Figure 5D). Flow cytometry detected over 90% of cells positive for pluripotent cell markers
251 expression: TRA-1-60, SSEA4, and OCT4 (Figure 5E and F). Further, G-band analysis revealed
252 that hiPSCs retained their normal karyotype even after three passages under large-scale
253 suspension conditions (Figure 5G). When large-scale suspension-culture derived hiPSCs were
254 incubated in each germ layer-specific differentiation medium for 4 - 7 days, the expression of
255 early differentiation markers for ectoderm (PAX6 and SOX1), mesoderm (T and PDGFRA) and

256 endoderm (SOX17 and CXCR4) was significantly induced (Figure 5H). These cells were then
257 directly differentiated into dopaminergic neural progenitors, cardiomyocytes, and hepatocytes to
258 evaluate their differentiation capacity and propensity. There were no differences in the
259 differentiation efficiency toward these lineages (Figure 5I-M). Hence, these results indicate that
260 the characteristics and quality of clinical-grade hiPSCs cultured in large-scale suspension
261 conditions in the presence of PKCβ and Wnt inhibitors were equivalent to those of hiPSCs
262 maintained under adherent conditions. Taken together, we were successful in mass suspension-
263 culture conditions supplemented with Wnt and PKCβ inhibitors.

264 **Single cell sorting and expansion of hiPSC subclones cultured in suspension conditions.**
265 We sorted a hiPSC line, 201B7, with TRA-1-60 antibody into individual wells of a 96-well plate
266 and attempted to establish subclones by expanding them with serial passages (Figure 6A). By day
267 28 after this single-cell sorting, we expanded single-cell-sorted hiPSC subclones in suspension
268 culture supplemented with IWR1-endo and LY3333531 (Figure 6B). On day 28, we examined
269 seven subclones for their cell growth and expression of OCT4 and TRA-1-60. The subclones
270 showed more than three million cells and high ratios of OCT4- and TRA1-60-positive cells
271 (Figure 6C-E). These results indicate that we have successfully derived single-cell-cloned
272 sublines in suspension culture.

273 **Direct freeze and thaw of hiPSCs cultured in suspension conditions.**
274 We froze a hiPSC line, 201B7, in suspension culture conditions supplemented with IWR1-endo
275 and LY3333531. Then, we thawed these frozen vials and directly reseeded the cells in suspension
276 conditions (Figure 6—figure supplement 1A). By day 10 after reseeding, we expanded the
277 hiPSCs in suspension culture supplemented with IWR1-endo and LY3333531 (Figure 6—figure
278 supplement 1B). On day 10, we examined three vials for their cell growth and expression of
279 OCT4 and TRA-1-60. The subclones showed more than three million cells and high ratios of
280 OCT4- and TRA1-60-positive cells (Figure 6—figure supplement 1C-E). These results indicate
281 that we have successfully frozen and thawed hiPSCs in suspension culture directly.

282 Together, these results suggest that the suspension culture conditions supplemented with Wnt and
283 PKCβ inhibitors are robust in harsh conditions such as single-cell expansion and freezing-and-
284 thaw processes.

285 **Establishment of hiPSC lines in complete suspension-culture conditions supplemented with**
286 **inhibitors of PKCβ and Wnt signaling pathways.**
287 For the clinical use of hiPSCs, more secure and efficient establishment of hiPSCs in closed
288 systems is strongly desired. To achieve this, we aimed to establish hiPSCs in suspension-culture
289 conditions. Using PBMCs as a starting material, we generated hiPSCs using a novel replication-
290 defective and persistent Sendai virus vector (SeVdp) infection or episomal vector electroporation,
291 as these methods are well-known for producing transgene-free, clinical-grade hiPSCs (Fusaki *et*

292 *al*, 2009; Nishimura *et al*, 2011) (Figure 7A). PMBCs were infected with SeVdp carrying OCT4,
293 SOX2, KLF4, and L-MYC. Infected cells were kept cultured by repeating passages every 5 - 6
294 days. Cell aggregates cultured with IWR1-endo and LY33351 showed uniform spherical structure
295 (Figure 7B), and most of the cells were positive for OCT4 (Figure 7C) and TRA-1-60 (Figure
296 7D) on day 56. These bulk cells were able to differentiate into three germ layers in an in vitro EB
297 formation assay (Figure 7E) and in teratomas that were transplanted into immunodeficient
298 NOD.Cg-Prkdcscid Il2rgtm1Wjl/SzJ (NSG) mice (Figure 7F). These bulk-hiPSCs maintained
299 normal karyotype (Figure 7G). By single cell sorting with fluorescent labeled TRA-1-60
300 antibody, we expanded single-cell-derived clones in suspension-culture conditions. A clone (F-
301 10) showed OCT4 and TRA1-60 expressions (Figure 7H-J). In addition, the established clone
302 showed potency to differentiate into derivatives of three germ layers *in vitro* as EBs (Figure 7K)
303 and *in vivo* as teratoma transplanted into NSG mice (Figure. 7L). A normal karyotype was
304 observed in this clone (Figure 7M). SeVdp was nearly extinct in these bulk populations and F-10
305 clone (Figure 7N). These results demonstrate that, we were successful in establishing transgene-
306 free hiPSC lines using SeVdp infection in suspension-culture conditions in the presence of PKCβ
307 and Wnt inhibitors.

308 Furthermore, we were successful in establishing single-cell-derived hiPSC lines using the
309 transfection of episomal plasmid vectors in suspension-culture conditions in the presence of
310 PKCβ and Wnt signaling inhibitors. PMBCs were transfected with episomal plasmid vector mix
311 carrying OCT4, SOX2, KLF4, L-MYC, LIN28, and mp53DD and cultured in suspension
312 conditions in the presence or absence of IWR-1-endo and LY33351 with repeated passages to
313 reach enough cell numbers to make cell stocks and characterization (Figure 7—figure supplement
314 1A). After 36 days of culture, 59% double positive cells for TRA-1-60 and SSEA4 were observed
315 in control, whereas 78% were seen in the presence of IWR-1-endo and LY333531 (Figure 7—
316 figure supplement 1B and C). We performed cell sorting of TRA-1-60 and SSEA4 double
317 positive cells and further repeated 5 more passages in the absence or presence of IWR-1-endo and
318 LY333531. Cell aggregates cultured in culture medium supplemented with IWR-1-endo and
319 LY333531 showed uniform spherical structures (Figure 7—figure supplement 1D), and the most
320 of these cells were TRA-1-60 and SSEA4 double positive (Figure 7—figure supplement 1E). In
321 contrast, cell aggregates cultured without these inhibitors showed lumpy, heterogeneous shapes,
322 and decreased undifferentiated population. Immunostaining of OCT4 on dissociated cell
323 aggregates resulted in higher OCT4 positive cells in IWR-1-endo and LY333531 treated cells
324 (Figure 7—figure supplement 1F and G). We further performed single cell sorting of TRA-1-60-
325 positive cells from bulk-cultured populations at 10 passages (Figure 7—figure supplement 1H
326 and I). We selected 3 clones to be characterized further. These clones showed round spherical
327 shapes in their aggregates and expression of OCT4, NANOG, and TRA-1-60 proteins (Figure 7—
328 figure supplement 1J-L). Pluripotency into three germ layers was confirmed in vitro with EB
329 formation assay (Figure 7—figure supplement 1M) and teratoma formation analysis (Figure.
330 Figure 7—figure supplement 1N). These clones retained a normal karyotype even after a long-

331 culture (Figure 7—figure supplement 1O). These results demonstrate that single-cell-derived
332 hiPSC lines were established using the transfection of episomal plasmid vectors in suspension-
333 culture conditions in the presence of PKCβ and Wnt signaling inhibitors.
334

335 **Discussion**

336 In this study, we have developed a series of methods to generate and maintain hiPSCs in
337 suspension conditions. First, we have identified compounds that suppress spontaneous
338 differentiation of hiPSCs in suspension cultures. Based on these findings, we have newly
339 achieved a complete series of culture processes including hiPSC establishment, long-term culture,
340 mass culture, single-cell cloning, and direct freeze and thaw (summarized in Table 1). These
341 methods require no special materials including microcarriers or dialysis bags, and are effective
342 with various existing culture media and many hiPSC lines. Therefore, this suspension-culture of
343 hiPSCs is anticipated to have novel industrial applications, which have been never achieved with
344 conventional methods because suspension-culture conditions, which precisely control cellular
345 states, have advantages in terms of mass culture, automation, and safety assurance.

346 We have identified two compounds as factors that ameliorate the disadvantages of the suspension
347 culture of hiPSCs. Wnt signaling inhibitors specifically inhibited differentiation toward
348 mesendoderm, whereas, the PKCβ inhibitor, LY333531, inhibited ectodermal differentiation and,
349 when combined with IWR-1-endo, maintained the undifferentiated nature of hiPSCs with high
350 efficiency. Go6983, a pan-PKC inhibitor, has been used to promote the self-renewal of
351 mammalian PSCs (Dutta *et al*, 2011; Kinehara *et al*, 2013; Rajendran *et al*, 2013; Takashima *et*
352 *al*, 2014); however, in these cases, the role of specific isoforms in PSC self-renewal and
353 differentiation are not fully elucidated yet. In this study, we demonstrated that PKCβ-specific
354 inhibitor LY333531 as well as Go6983 showed the suppression of neuroectodermal
355 differentiation. Interestingly, these combinations of chemical inhibitors against WNT and PKC
356 signaling pathways are also being used in the induction and maintenance of naive human
357 pluripotent stem cells (Bayerl *et al*, 2021; Bredenkamp *et al*, 2019; Guo *et al*, 2017; Khan *et al*,
358 2021). While, in suspension-culture, we did not aim to drive hiPSCs to a naïve state by the use of
359 these combinations of chemical inhibitors conditions, it would be worthwhile to investigate the
360 effect of adaptation of suspension-culture supplemented with PKCβ and Wnt signaling inhibitors
361 on the transition of the naïve PSCs types.

362 We successfully generated hiPSC lines from PBMCs in suspension conditions for the first time
363 by adding the abovementioned compounds to the culture medium. Both transduction methods
364 with SeVdp and episomal plasmid vectors enabled the establishment of hiPSCs under suspension
365 conditions in the presence of IWR-1-endo and LY333531. Clonal expansion of hiPSCs was also
366 performed by single-cell sorting with flow cytometry and were successfully characterized for
367 their self-renewal, pluripotency, and genomic integrity. These results indicate that hiPSC lines
368 generated in suspension conditions have the same quality in terms of their pluripotency, self-
369 renewal, and genomic integrity as those generated with conventional adherent conditions. Precise
370 control of hiPSC status in suspension culture could pave the way for their stable and automated
371 clinical application toward autologous cell therapy of hiPSCs.
372

373 **Methods**
374
375 **Human subjects**
376 The generation and use of hiPSCs were approved by the Ethics Committee of RIKEN
377 BioResource Research Center, Graduate School of Medicine of Kyoto University, and KANEKA
378 CORPORATION.
379
380 **Animal experiments**
381 All animal experiments were approved by the Animal Experimentation Committee of the RIKEN
382 Tsukuba branch and were performed according to the committee's guiding principles and the
383 "Guide for the Care and Use of Laboratory Animals" published by the National Institute of
384 Health.
385
386 **Data availability**
387 All data are available in the main text or the supplementary materials. RNA-seq data are available
388 in the Gene Expression Omnibus as GSE222833. All the data supporting the findings of this
389 study are available from the lead contact upon reasonable request. Source data is provided with
390 this paper. This paper does not report original code.
391
392 **HiPSCs cultured in adherent conditions**
393 WTC11 (GM25256 from Coriell Institute) (Hayashi *et al*, 2016), 201B7 (HPS0063 from RIKEN
394 Cell Bank) (Takahashi *et al*., 2007), 454E2 (HPS0077 from RIKEN Cell Bank) (Okita *et al*,
395 2011), 1383D6 (HPS1006 from RIKEN Cell Bank) (Okita *et al*., 2011), 1231A3 (HPS0381 from
396 RIKEN Cell Bank) (Okita *et al*., 2011), and Ff-I14s04 (CiRA foundation, Kyoto University)
397 (Kitano *et al*., 2022) were used as healthy-donor hiPSC lines. With tdTomato-reporter hiPSC
398 lines, we generated knock-in hiPSC lines for PAX6-TEZ (constructed from 454E2 line) and
399 SOX17-TEZ (constructed from 1383D6 line) using CRISPR-Cas9 genome editing (Tsukamoto *et*
400 *al*, 2021) (Figure. S1A). These hiPSCs were cultured in StemFit AK02N medium (Cat#AK02N,
401 Ajinomoto, Co., Ltd., Tokyo, Japan). Medium change was performed every day and passaged at
402 80%–90% confluency after 6-7 days of culture. At passage, PBS/EDTA solution (0.5 mM,
403 Cat#06894-14, Nacalai Tesque) was used to dissociate hiPSC colonies, and these cells were
404 seeded at a density of 2,500 cells/cm^2. 10 μM Y-27632 (Cat#HY-10071, FUJIFILM Wako Pure
405 Chemical Corporation, Osaka, Japan) and 0.25 μg/cm^2 iMatrix-511 silk (Cat#892021, Matrixome
406 Inc, Osaka, Japan) were added to the culture dish on seeding day.
407
408 **Suspension-culture of hiPSCs**
409 Suspension culture with rotation at 90 rpm was performed with a plate shaker (Cat#WB-101SRC,
410 WAKENBTECH, Kyoto, Japan or #0081704-000, TAITEC, Tokyo, Japan) installed in a CO_2

411 incubator (Cat#Steri-Cycle i160, Thermo Fisher Scientific, MA, USA) and operated under high
412 humidity continuously during the whole culture period. To start the culture hiPSCs in suspension
413 conditions, 4×10^5 cells were seeded in one well of a low-attachment 6-well plate (Cat#MS-
414 80060, Sumitomo Bakelite, Tokyo, Japan) with 4 mL of StemFit AK02N medium,
415 StemFitAK03N (Cat#AK03N, Ajinomoto, Co., Ltd., Tokyo, Japan), or StemScale PSC
416 suspension medium (A4965001, Thermo Fisher Scientific, MA, USA) supplemented with 10 μM
417 Y-27632. This plate was placed onto the plate shaker in the CO_2 incubator. The medium without
418 Y-27632 was changed every day unless otherwise specified. On days 3 - 5, the hiPSC aggregates
419 were dissociated with Accutase (Cat#12679-54, Nacalai Tesque) at 37°C for 10 min and used for
420 the next suspension-culture. This passage was performed every 5 days unless otherwise specified.
421 To screen for factors that inhibit spontaneous differentiation of hiPSCs, chemicals or recombinant
422 proteins were added to the culture medium (listed in Supplementary Table S1).
423
424 **Bioreactor culture of hiPSCs**
425 A frozen stock of hiPSCs was pre-cultured twice in adherent conditions to prepare enough cell
426 numbers. To prepare enough hiPSCs to start large-scale culture, hiPSCs were pre-cultured in
427 iMatrix-511MG (Cat#892 005, Matrixome, Inc, Osaka, Japan) or Vitronectin (VTN-N)
428 Recombinant Human Protein, Truncated (Cat#A14700, Thermo Fisher Scientific, MA, USA)-
429 coated cell culture flasks with StemFit AK03N medium including 20 μM IWR-1-endo and 1 μM
430 LY333531. Perfusion-culture was started with $3.2 - 4.8 \times 10^7$ cells in 320 mL of StemFit AK03N
431 medium (Cat#AK03N, Ajinomoto, Tokyo, Japan) with IWR-1-endo and LY333531. The reactor
432 system BioFlo320 (Eppendorf, Hamburg, Germany) was used for large-scale hiPSCs culture. To
433 maintain the lactate concentration below a certain level and to regulate the pH, the culture was
434 carried out by increasing the amount of medium perfusion per unit time in accordance with the
435 cell proliferation transition. To prevent pH decrease, CO_2 concentration was regulated by
436 feedback control in the reactor system. After 3-4 days of culture, the formed hiPSC aggregates
437 were dissociated with TrypLE SELECT (Cat#A12859-01, Thermo Fisher Scientific, MA, USA)
438 collected for making cell stocks (~300 tubes). This perfusion culture was repeated three times
439 (P1, P2, and P3) and the cells were prepared at each expansion step.
440
441 **HiPSC generation in suspension culture conditions**
442 HiPSCs were generated from healthy donor-derived PBMCs (Precision for Medicine). Thawed
443 PMBCs from a vial containing around 1×10^7 cells were pre-cultured in one well of low
444 attachment 6-well plate including 4 mL of StemSpan-AOF (Cat#ST100-0130, STEMCELL
445 Technologies, Vancouver, Canada) supplemented with recombinant human IL-6 (100 ng/mL),
446 IL-3 (10 ng/mL), SCF (300 ng/mL), TPO (300 ng/mL), and FLT3 ligand (300 ng/mL) (all from
447 FUJIFILM Wako Pure Chemical Corporation, Tokyo Japan). After 24 h of incubation with
448 continuous stirring at 37°C and 5% CO_2, PBMCs were spun down with centrifugation at 200 × g
449 for 10 min at low deceleration speed and resuspended in StemSpan ACF for cell counting. 2.5 ×

450 10^6 cells of PMBCs were centrifuged at 200 × g for 10 min with low deceleration speed, and
451 electroporated using Nucleofector 2b device (Lonza, Basel, Switzerland) with iPS cell Generation
452 Episomal vector Mix (Takara Bio, Shiga, Japan) and Amaxa Human $CD34^+$ Cell Nucleofector kit
453 (Lonza, Basel, Switzerland) according to manufacturer's protocol. 5×10^5 of electroporated cells
454 were seeded in one well of a low attachment 6-well plate in 4 mL StemSpan ACF with the
455 cytokines mentioned above. Suspension-culture was performed with continuous agitation at 90
456 rpm. Stem span ACF medium were gradually replaced with StemFit AK02N medium. Formed
457 cell aggregates were passaged with Accutase on day 16 in the presence of 10 μM Y27632, and
458 suspension-culture was continued until the cell numbers reached a sufficient amount for
459 characterization. 10 μM IWR-1-endo and 1 μM LY333531 were added from day 3.
460 SeVdp infection was performed with Sendai Reprogramming Kit (CytoTune EX-iPS of
461 virus solution, ID Pharma, Tsukuba, Japan) according to the manufacturer's protocol with some
462 modifications. Briefly, pre-cultured 1×10^6 PMBCs were centrifuged at 200 × g for 10 min, with
463 low deceleration speed, and resuspended in 2 mL of StemSpan ACF with cytokines. PMBCs were
464 gently mixed with 2 mL of virus solution prepared at MOI = 5 per 1×10^6 cells. 5×10^5 infected
465 cells were seeded in one well of low-attachment 6-well plate at a total volume of 4 mL with
466 StemSpan ACF plus cytokines. Suspension-culture was initiated with continuous agitation at 90
467 rpm. Stem span ACFs were gradually replaced with StemFit AK02N as mentioned above, and the
468 cell aggregates were passaged with Accutase on day 16 in the presence of 10 μM Y-27632.
469 Suspension-culture and passages continued until cell reached a sufficient number for
470 characterization. 10 μM IWR-1-endo and 1 μM LY333531 were added from day 23.
471
472 **Three germ layer differentiation *in vitro***
473 For Embryoid body (EB) formation assay, suspension-cultured hiPSC lines were dissociated with
474 Accutase and 1.0 x 10^4 cells were seeded in each well of an EZ-BindShut 96-well-V plate
475 (Cat#4420-800SP AGC TECHNO GLASS CO., LTD, Shizuoka, Japan) with 100 μL Stem Fit
476 AK02N medium supplemented with 10 μM Y-27632. Before culture, the 96-well-V plate was
477 centrifuged at 200 x g for 3 min for efficient cell mass formation. The next day, the culture
478 medium was switched to DMEM high Glucose (Cat#08458-16, Nacalai tesque, Kyoto, Japan)
479 supplemented with 10% fetal bovine serum (here after referred as EB medium). On day 8, EBs
480 were transferred into 0.1% (w/v) Gelatin Solution (Cat#190–15805, FUJIFILM Wako Pure
481 Chemical Corporation, Tokyo Japan) -coated 12-well plate and further cultured in EB medium for
482 another 8 days. The medium was changed every day. EBs were fixed with 4% paraformaldehyde
483 in Dulbecco's Phosphate Buffered Saline (D-PBS) (Cat#14249-24, Nacalai tesque, Kyoto, Japan)
484 for 10 min at room temperature and used for immunostaining. Differentiation was validated by
485 immunostaining against each germ layer markers.
486 The differentiation potency of suspension-cultured hiPSCs toward three germ layers was
487 also evaluated by culturing in germ layer specific differentiation medium. For ectodermal
488 differentiation, suspension-cultured hiPSCs spheroids were cultured with Stem Fit AK02N

489 without C medium supplemented with 10 μM SB431542 (Cat#198-16543, FUJIFILM Wako Pure
490 Chemical Corporation, Tokyo, Japan) and 10 μM DMH1 (Cat#041-33881FUJIFILM Wako Pure
491 Chemical Corporation, Tokyo, Japan) for 7 days. For mesodermal differentiation, suspension-
492 cultured hiPSCs spheroids were cultured with RPMI1640 medium (FUJIFILM Wako Pure
493 Chemical Corporation, Tokyo, Japan) supplemented with B-27 supplement, minus insulin
494 (A1895601, Thermo Fisher Scientific, MO, USA) and 7.5 μM CHIR99021 (Cat#034-23103,
495 FUJIFILM Wako Pure Chemical Corporation, Tokyo, Japan) for 1 day, and continuously with
496 RPMI1640 medium supplemented with B-27 supplement for 2 days. For endodermal
497 differentiation, suspension-cultured hiPSCs spheroids were cultured with RPMI1640 medium
498 supplemented with 1 mM Sodium pyruvate (FUJIFILM Wako Pure Chemical Corporation,
499 Tokyo, Japan), 1 x NEAA (FUJIFILM Wako Pure Chemical Corporation, Tokyo, Japan), 80
500 ng/mL Activin A (R&D Systems, MN, USA), 55 μM 2-mercaptethanol (FUJIFILM Wako Pure
501 Chemical Corporation, Tokyo, Japan), 50 ng/mL FGF2 (R&D Systems, MN, USA), 20 ng/mL
502 BMP4, and 3 μM CHIR99021 for 2 days, and continuously with RPMI1640 medium
503 supplemented with 1 mM Sodium pyruvate, 1× NEAA, 80 ng/mL Activin A, 55 μM 2-
504 mercaptethanol, and 0.5% Knockout serum replacement (KSR; Thermo Fisher Scientific, MO ,
505 USA) for 2 days.
506
507 **Neuroectoderm and endoderm differentiation of reporter hiPSC lines**
508 Reporter hiPSC lines, PAX6-TEZ and SOX17-TEZ were used as positive controls for in vitro
509 neuroectoderm and endoderm differentiation, respectively. PAX6-TEZ was seeded in each well
510 of a 24 well-plate coated with 0.25 μg/cm^2 iMatrix-511 silk with 1 mL StemFit AK02N medium
511 supplemented with 10 μM Y-27632. Next day, the culture medium was switched to Stem Fit
512 AK02N medium without supplement C, instead of containing 10 μM SB431542 and 10 μM
513 DMH1. SOX17-TEZ was seeded in each well of a 24 well-plate (same as above), and on the next
514 day, the culture medium was switched to StemFit AK02N medium without supplement C instead
515 of containing 3 μM CHIR99021 and 10 ng/mL Activin A (Cat#014-23961, FUJIFILM Wako
516 Pure Chemical Corporation, Tokyo, Japan). The medium was changed every day. On day 7,
517 tdTomato expression was observed under all-in-one fluorescent microscope (BZ-X800;
518 KEYENCE).
519
520 **Cardiomyocyte differentiation**
521 Cardiomyocyte differentiation was performed according to a modified method described
522 previously (Funakoshi *et al*, 2016). Both large-scale suspension cultured hiPSCs and typical
523 adherent-cultured hiPSC were collected by centrifugation after dissociation into single cell with
524 TrypLE Select. The cells were suspended in 1.5 mL cardiomyocyte differentiation media (CDM),
525 consisting of StemPro34 medium (Thermo Fisher Scientific) supplemented with 2 mM Glutamax
526 (Thermo Fisher Scientific), 50 μg/mL ascorbic acid, 4×10^{-4} M monothioglycerol (Sigma-
527 Aldrich), 150 μg/mL transferrin (Roche), and with Matrigel (Cat#354277, Corning, NY, USA)),

528 10 μM Y-27632 and 2 ng/mL human recombinant BMP4 (R&D Systems) and then cultured in
529 ultra-low attachment 6 well plate (Corning) in 5%CO_2/5% O_2. After 24 h, 1.5 mL CDM with
530 6 ng/mL human recombinant activin A (R&D Systems) and 5 ng/mL bFGF (R&D Systems) were
531 added into the wells. After 3 days, medium was changed to 3 mL CDM with 10 ng/mL VEGF
532 (R&D Systems), SB431542 (Sigma-Aldrich), Dorsomorphin (Sigma-Aldrich) and 1 μM IWP-3
533 (Stemgent). After 7 days, medium was changed to 3 mL CDM with 10 ng/mL VEGF (R&D
534 Systems). The medium was changed every 2 days. The cells were collected at 15 days after
535 differentiation and analyzed by flow cytometry.
536
537 **Dopaminergic progenitor cells differentiation**
538 Dopaminergic progenitor cells differentiation was performed according to a modified method
539 described previously (Doi *et al*, 2020). Both large-scale suspension cultured hiPSCs and typical
540 adherent-cultured hiPSC were collected by centrifugation after dissociation into single cell with
541 TrypLE Select. The cells were suspended in 1 mL dopaminergic progenitor cells differentiation
542 medium-1 (DPM-1), consisting of Glasgow's minimum essential medium (Thermo Fisher)
543 supplemented with 8% knockout serum replacement (Thermo Fisher Scientific), 1% MEM Non-
544 Essential Amino Acids Solution (Thermo Fisher Scientific), 1 mM sodium pyruvate (Sigma-
545 Aldrich), 0.1 mM 2-mercaptoethanol (FujiFilm Wako) and 100 nM LDN193189 (Stemgent), and
546 were then seeded in iMatrix-coated 24-well plates at a density of 1×10^6 cells/well with 10 μM Y-
547 27632 and 500 nM A-83-01 (FujiFilm Wako). After 1 and 2 days, medium was changed to DPM-
548 1 with 500 nM A-83-01, 100 ng/mL recombinant human FGF8 (FujiFilm Wako), and 2 μM
549 purmorphamine (FujiFilm Wako). After 3 to 6 days, medium was changed every day to DPM-1
550 with 500 nM A-83-01, 100 ng/mL recombinant human FGF8, 2 μM purmorphamine, and 3 μM
551 CHIR99021 (FujiFilm Wako). After 7 to 11 days, medium was changed every day to DPM-1
552 with 3 μM CHIR99021. On differentiation day 12, cells were dissociated using TrypLE select
553 and suspended in the dopaminergic progenitor cells differentiation medium-2 (DPM-2),
554 consisting Neurobasal medium (Thermo Fisher Scientific), 2% B27 supplement (without Vitamin
555 A, Thermo Fisher), 1% GlutaMAX (Thermo Fisher Scientific), 10 ng /mL human recombinant
556 glial cell-derived neurotrophic factor (FujiFilm Wako), 200 mM ascorbic acid, 20 ng / mL human
557 recombinant brain-derived neurotrophic factor (FujiFilm Wako), and 400 μM dibutyryl cAMP
558 (FujiFilm Wako), and were then plated on U-shaped 96-well plates (Thermo Fisher Scientific) at
559 a density of 2×10^4 cells/150 μL/well with 10 μM Y-27632. After 15 to 26 days, half of medium
560 was changed every 2 days to DPM-2. Dopaminergic progenitor cells differentiation efficiency
561 was analyzed by flow cytometry at 12 days after differentiation. On differentiation day 12, cells
562 were labeled with anti-CORIN antibody (Clone 5B6, Sigma-Aldrich) and secondary antibody
563 (A11001, Thermo Fisher).
564
565 **Hepatocyte differentiation**

566 Hepatocyte differentiation was performed according to a modified method described previously
567 (Si-Tayeb *et al*, 2010). Both large-scale suspension-cultured and typical adherent-cultured hiPSCs
568 were collected by centrifugation after dissociation into single cell with TrypLE Select. These
569 hiPSCs were cultured on Matrigel-coated 6-well plates until 80% confluency with StemFit
570 medium (Ajinomoto). To initiate differentiation, the medium was changed to 1 mL Hepatocyte
571 differentiation medium (HDM) consisting of RPMI1640 medium (Thermo Fisher) supplemented
572 with 1× GlutaMax (Thermo Fisher) and 1× B27 Supplement minus vitamin A, with the addition
573 of 100 ng/mL Activin A (R&D Systems). After 1 to 3 days, medium was changed every day to
574 HDM with 100 ng/mL Activin A. After 4 to 8 days, medium was changed every day to HDM
575 with 20 ng/mL human recombinant BMP-4 (R&D Systems) and 20 ng/mL human recombinant
576 FGF-4 (R&D Systems). After 9 to 13 days, medium was changed every day to HDM with 20
577 ng/mL human recombinant HGF (R&D Systems). After 14 to 24 days, medium was changed
578 every 2 days to Hepatocyte Culture Medium (HCM; Lonza) with 20 ng/mL human recombinant
579 Oncostatin M (R&D Systems). On differentiation day 25, the albumin concentration in the culture
580 supernatant was determined by ELISA using an anti-human albumin antibody (Betyl
581 Laboratories, Catalog # E88-129).
582
583 **Teratoma formation**
584 Suspension-cultured hiPSCs were dissociated with Accutase and then resuspended with 1 mL of
585 StemFit AK02N medium supplemented with 10 μM Y-27632. 1 x 10^6 cells were collected by
586 centrifugation at 200 × g for 3 m and suspended in ice-cold 50% Matrigel solution: StemFit
587 AK02N with 10 μM Y-27632 = 1:1). Cells were injected into testis or leg of NOD.Cg-Prkdcscid
588 Il2rgtm1Wjl/SzJ (NSG) mice (The Jackson Laboratory, Bar Harbor, ME, USA) using an 18-G
589 needle. Two to three months later, teratomas were collected and fixed with 4% paraformaldehyde
590 in D-PBS. Paraffin-embedded sectioning and hematoxylin-eosin (HE) staining was performed.
591 Three germ layer derivatives were observed under CKX53 microscope with a DP22 camera and
592 CellSens software (EVIDENT, Tokyo, Japan).
593
594 **Karyotyping**
595 For virtual karyotyping, genomic DNA (gDNA) was extracted from hiPSCs using a DNeasy
596 Blood & Tissue Kit (Cat#69504, QIAGEN, Hulsterweg, Netherland) and was used for microarray
597 assay. Virtual karyotyping was performed with GeneChip Scanner System 3000 using Karyostat
598 Assay arrays (Cat#905403, both from Thermo Fisher Scientific, MA, US) according to the
599 manufacturer's protocol. Data were analyzed using the Chromosome Analysis Suite (ChAS) and
600 Affymetrix GeneChip Command Console software programs.
601 G-band analysis was performed using the common Giemsa staining method with hiPSCs
602 fixed by Carnoy's fixtative (3:1 ratio of methanol: glacial acetic acid).
603
604 **qRT-PCR**

605 Total RNA was extracted with a FastGene RNA premium kit (Cat#FG-81250, NIPPON Genetics,
606 Tokyo, Japan) and used for reverse transcription reaction. cDNA was synthesized by using a
607 ReverTra Ace qPCR RT kit (Cat#FSQ-101, TOYOBO, Osaka, Japan) with random primers.
608 Real-Time qPCR reactions were performed with a QuantStudio 3 System (Thermo Fisher
609 Scientific) using THUNDERBIRD Probe qPCR Mix (Cat#QPS-101, TOYOBO) with TaqMan
610 probes (listed in Supplementary Table 2) (Thermo Fisher Scientific) according to the
611 manufacturer's instructions. Gene expression was described as the fold change relative to the
612 control sample value (ΔΔCt method) after normalization to the corresponding GAPDH or β-
613 Actin values, unless otherwise specified. For the residual SeV detection, data were normalized to
614 the expression of GAPDH and displayed as relative fold increase to hiPSC line established with
615 episomal vector (WTc11). SeVdp-infected fibroblasts on passage 1 (SeV-34 and -39) were used
616 as positive controls.
617
618 **Immunocytochemistry**
619 Immunocytochemistry was performed on adherent cells. Suspension-cultured hiPSCs were
620 dissociated with Accutase and transiently cultured as adherent in iMatrix-coated culture dishes for
621 3 h before immunocytochemistry. The cells were fixed with 4% paraformaldehyde in D-PBS for
622 10 min at room temperature, then permeabilized in D-PBS containing 0.1% Triton X-100 for
623 another 10 min. Cells were incubated with primary antibodies in D-PBS containing 0.1% Bovine
624 Serum Albumin (BSA; Cat#017-22231, FUJIFILM Wako Pure Chemical Corporation, Tokyo,
625 Japan) overnight at 4 °C. The secondary antibodies were incubated for 1 hour at room
626 temperature in D-PBS containing 0.1% BSA. Fluoro-KEEPER Antifade Reagent, Non-Hardening
627 Type with DAPI (Cat#12745-74, Nacalai tesque, Kyoto, Japan) was used for nuclear
628 counterstaining. Fluorescence images were taken with an all-in-one fluorescent microscope (BZ-
629 X800; KEYENCE, Osaka, Japan). The primary and secondary antibodies used in this study are
630 listed in Supplementary Tables 3 and 4, respectively.
631
632 **Automatic capillary Western blot (Simple Western Assays)**
633 To detect the expression of PAX6 or SOX17, adherent- or suspension-cultured PAX6-TEZ or
634 SOX17-TEZ hiPSCs were collected on day 10 (Passage 2). The cell lysate was prepared from 1 ×
635 10^6 cells with sodium dodecyl sulfate-polyacrylamide gel electrophoresis (SDS-PAGE) sample
636 buffer solution without 2-ME (2x) (Cat#30567-12, Nacalai Tesque) supplemented with 100 mM
637 Dithiothreitol (DTT) (Cat#14130-41, Nacalai Tesque). To detect phosphorylated PKCβ, cell
638 lysates were collected on day 5 of suspension-cultured hiPSCs with extraction buffer mentioned
639 above, containing 1% phosphatase inhibitor cocktail (Cat#07574-61, Nacalai Tesque). Samples
640 were denatured at 95°C for 5 min. Western blotting was performed with a capillary automatic
641 western blotting device (Simple Western, Wes; Bio-Techne, CA, USA). Jes/Wes 12- to 230-kDa
642 separation module for Wes, 8 × 25 capillary cartridges (Cat#SM-W004, ProteinSimple), and
643 Anti-Rabbit/Goat/Mouse Detection Module kit (Cat#DM-002/DM-001/DM/006, ProteinSimple)

644 were used. Preparation of reagents and sample loading were conducted according to the
645 manufacturer's instructions. The data were analyzed and quantified by compass for simple
646 Western software program (ProteinSimple). GAPDH was used as the reference for normalization.
647 The primary antibodies used in this study are listed in Supplementary Table 3.
648
649 **Flow cytometry**
650 Flow cytometry of self-renewal markers, TRA-1-60 and SSEA4 was performed as described in
651 our previous study. Briefly, adherent- or suspension-cultured hiPSCs were dissociated with 0.5
652 mM EDTA solution in D-PBS or Accutase, respectively. Dissociated cells (0.5 or 1×10^6 cells)
653 were collected and centrifuged at 200 × g for 3 minutes and resuspended in 500 or 1000 μL PBS
654 containing 0.1% BSA and 0.5 mM EDTA, then incubated with or without anti-TRA-60 antibody
655 or anti-SSEA4 antibody for 1 hour at 4 °C under oblique light conditions. After washing with
656 PBS, cells were resuspended in 500 mL D-PBS containing 0.1% BSA and 0.5 mM EDTA, and
657 filtrated with 35-mm cell strainer (Cat#352235, FALCON, Thermo Fisher Scientific). For PAX6-
658 TEZ and SOX17-TEZ hiPSC lines, adherent- or suspension-cultured hiPSCs were dissociated
659 into single cells and collected cells were resuspended in 500 mL PBS containing 0.1% BSA and
660 0.5 mM EDTA. After passing through the 35-mm cell strainer, cells were analyzed for tdTomato.
661 The primary and secondary antibodies used in this study are listed in Supplementary Table 3 and
662 4, respectively. Flow cytometry was performed with SH800 cell Sorter (SONY, Tokyo, Japan).
663
664 **RNA-Seq**
665 Total RNA was extracted using the FastGene RNA premium kit, and strand-specific library
666 preparation was performed. The prepared library was sequenced using a NovaSeq6000 (Illumina,
667 Inc, CA, USA). Sequencing was performed in a 150 bp × 2 paired-end conFigureuration with a
668 data output of about 6 Gb per sample (~ 20 million paired reads). Library preparation and
669 sequencing was performed in GENEWIZ (Azenta, MA, USA). To identify differentially
670 regulated genes, sequencing data was analyzed with a CLC Genomics Workbench (QIAGEN,
671 Hulsterweg, the Neterlands) and R package, edgeR (v3.30.3) in R language (v 4.1.0). An MA plot
672 (log2 fold change versus mean average expression) comparing transcriptomes between
673 suspension- and adherent-culture from RNA-seq data. Transcripts with log2 fold change $\geqq 2$ or $\leqq$
674 -2 (FDR <0.01) are highlighted with red and blue dots, respectively. The extracted genes were
675 analyzed for gene ontology enrichment and biological pathways using the R package,
676 clusterProfiler (v3.16.1). GSEA was also performed using clusterProfiler. An enrichment map
677 was used to visualize the GSEA results with enrichment score (ES) and false discovery rate
678 (FDR) values. Software used for the analysis is listed in Supplementary Table 5.
679
680 **Statistical analysis**
681 Statistical analysis was performed using Student's t-test or Dunnett's test for multiple
682 comparisons with a single control condition. P values < 0.05 were considered statistically

683 significant. *, ** or *** in the graphs indicate $P<0.05$, $P<0.01$ or $P<0.001$, respectively. No
684 statistical methods were used to predetermine sample size. The experiments were not randomized
685 and the investigators were not blinded to allocation during experiments and outcome assessment.
686

Acknowledgments

We thank Dr. Bruce Conklin for providing us with the WTC11 hiPSC line; Dr. Shinya Yamanaka, Dr. Kazutoshi Takahashi, Dr. Masato Nakagawa, and Dr. Keisuke Okita for providing us with 201B7, 454E2, 1231A3, 1383D6, and Ff-I14s04 hiPSC lines. We would like to express our sincere gratitude to Dr. Kaoru Saijo, Mr. Daiki Kondo and Mr. Masahiko Yamada for their technical assistance, and Ms. Kumiko Omori for her administrative support. This work was funded by a collaborative research grant from Kaneka corporation. We would like to thank Editage [http://www.editage.com] for editing and reviewing this manuscript for English language.

Author Contributions: Conceptualization: YHA, Methodology: MMT, SK, CW, KT,MI, YHA, Investigation: MMT, SK, YHE, TW, TS, YA, KT, MI, MN, MU, TMK, MN, KN, YN, YHA, Visualization: MMT, SK, TS, YH, Funding acquisition: MMT, TN, YK, YHA, Project administration: MMT, TN, YK, YHA, Supervision: MMT, TN, YN, NT, YK, YHA, Writing – original draft: MMT, KS, MT, YHA, Writing – review & editing: MMT, YHA

Competing Interest Statement: Y. HA received collaborative research grant from KANEKA corporation during this study. S. K., K.T., M. I., Y.K., and T.N. were employed with KANEKA corporation during this study. M.M.T., S.K. K.T., M. I., Y.K., and Y.HA. are inventors of patents arising from this work (WO/2021/162090 and PCT/JP2020/005255). The other authors declare no competing interests.

Classification: Applied Biological Sciences, Cell Biology, and Developmental Biology in BIOLOGICAL SCIENCES

Keywords: induced pluripotent stem cells (iPSCs), suspension culture, spontaneous differentiation, Protein Kinase C (PKC), WNT

710 **References**

711 Amit M, Chebath J, Margulets V, Laevsky I, Miropolsky Y, Shariki K, Peri M, Blais I, Slutsky
712 G, Revel M *et al* (2010) Suspension culture of undifferentiated human embryonic and induced
713 pluripotent stem cells. *Stem Cell Rev Rep* 6: 248-259
714 Amit M, Laevsky I, Miropolsky Y, Shariki K, Peri M, Itskovitz-Eldor J (2011) Dynamic
715 suspension culture for scalable expansion of undifferentiated human pluripotent stem cells. *Nat*
716 *Protoc* 6: 572-579
717 Bayerl J, Ayyash M, Shani T, Manor YS, Gafni O, Massarwa R, Kalma Y, Aguilera-Castrejon A,
718 Zerbib M, Amir H *et al* (2021) Principles of signaling pathway modulation for enhancing human
719 naive pluripotency induction. *Cell Stem Cell* 28: 1549-1565 e1512
720 Bredenkamp N, Yang J, Clarke J, Stirparo GG, von Meyenn F, Dietmann S, Baker D, Drummond
721 R, Ren Y, Li D *et al* (2019) Wnt Inhibition Facilitates RNA-Mediated Reprogramming of Human
722 Somatic Cells to Naive Pluripotency. *Stem Cell Reports* 13: 1083-1098
723 Chen B, Dodge ME, Tang W, Lu J, Ma Z, Fan CW, Wei S, Hao W, Kilgore J, Williams NS *et al*
724 (2009) Small molecule-mediated disruption of Wnt-dependent signaling in tissue regeneration
725 and cancer. *Nat Chem Biol* 5: 100-107
726 Chen KG, Mallon BS, McKay RD, Robey PG (2014) Human pluripotent stem cell culture:
727 considerations for maintenance, expansion, and therapeutics. *Cell Stem Cell* 14: 13-26
728 Dang SM, Gerecht-Nir S, Chen J, Itskovitz-Eldor J, Zandstra PW (2004) Controlled, scalable
729 embryonic stem cell differentiation culture. *Stem Cells* 22: 275-282
730 Doi D, Magotani H, Kikuchi T, Ikeda M, Hiramatsu S, Yoshida K, Amano N, Nomura M,
731 Umekage M, Morizane A *et al* (2020) Pre-clinical study of induced pluripotent stem cell-derived
732 dopaminergic progenitor cells for Parkinson's disease. *Nat Commun* 11: 3369
733 Dutta D, Ray S, Home P, Larson M, Wolfe MW, Paul S (2011) Self-renewal versus lineage
734 commitment of embryonic stem cells: protein kinase C signaling shifts the balance. *Stem Cells*
735 29: 618-628
736 Dziedzicka D, Tewary M, Keller A, Tilleman L, Prochazka L, Ostblom J, Couvreu De
737 Deckersberg E, Markouli C, Franck S, Van Nieuwerburgh F *et al* (2021) Endogenous suppression
738 of WNT signalling in human embryonic stem cells leads to low differentiation propensity towards
739 definitive endoderm. *Sci Rep* 11: 6137
740 Elanzew A, Sommer A, Pusch-Klein A, Brustle O, Haupt S (2015) A reproducible and versatile
741 system for the dynamic expansion of human pluripotent stem cells in suspension. *Biotechnol J*
742 10: 1589-1599
743 Funakoshi S, Miki K, Takaki T, Okubo C, Hatani T, Chonabayashi K, Nishikawa M, Takei I,
744 Oishi A, Narita M *et al* (2016) Enhanced engraftment, proliferation, and therapeutic potential in
745 heart using optimized human iPSC-derived cardiomyocytes. *Sci Rep* 6: 19111

746 Fusaki N, Ban H, Nishiyama A, Saeki K, Hasegawa M (2009) Efficient induction of transgene-
747 free human pluripotent stem cells using a vector based on Sendai virus, an RNA virus that does
748 not integrate into the host genome. *Proc Jpn Acad Ser B Phys Biol Sci* 85: 348-362
749 Gschwendt M, Dieterich S, Rennecke J, Kittstein W, Mueller HJ, Johannes FJ (1996) Inhibition
750 of protein kinase C mu by various inhibitors. Differentiation from protein kinase c isoenzymes.
751 *FEBS Lett* 392: 77-80
752 Guo G, von Meyenn F, Rostovskaya M, Clarke J, Dietmann S, Baker D, Sahakyan A, Myers S,
753 Bertone P, Reik W *et al* (2017) Epigenetic resetting of human pluripotency. *Development* 144:
754 2748-2763
755 Hayashi Y, Furue MK (2016) Biological Effects of Culture Substrates on Human Pluripotent
756 Stem Cells. *Stem Cells Int* 2016: 5380560
757 Hayashi Y, Hsiao EC, Sami S, Lancero M, Schlieve CR, Nguyen T, Yano K, Nagahashi A, Ikeya
758 M, Matsumoto Y *et al* (2016) BMP-SMAD-ID promotes reprogramming to pluripotency by
759 inhibiting p16/INK4A-dependent senescence. *Proc Natl Acad Sci U S A* 113: 13057-13062
760 Horiguchi I, Sakai Y (2016) Serum replacement with albumin-associated lipids prevents excess
761 aggregation and enhances growth of induced pluripotent stem cells in suspension culture.
762 *Biotechnol Prog* 32: 1009-1016
763 Hunt MM, Meng G, Rancourt DE, Gates ID, Kallos MS (2014) Factorial experimental design for
764 the culture of human embryonic stem cells as aggregates in stirred suspension bioreactors reveals
765 the potential for interaction effects between bioprocess parameters. *Tissue Eng Part C Methods*
766 20: 76-89
767 Ibuki M, Horiguchi I, Sakai Y (2019) A novel tool for suspension culture of human induced
768 pluripotent stem cells: Lysophospholipids as a cell aggregation regulator. *Regen Ther* 12: 74-82
769 Jirousek MR, Gillig JR, Gonzalez CM, Heath WF, McDonald JH, 3rd, Neel DA, Rito CJ, Singh
770 U, Stramm LE, Melikian-Badalian A *et al* (1996) (S)-13-[(dimethylamino)methyl]-10,11,14,15-
771 tetrahydro-4,9:16, 21-dimetheno-1H, 13H-dibenzo[e,k]pyrrolo[3,4-
772 h][1,4,13]oxadiazacyclohexadecene-1,3(2H)-d ione (LY333531) and related analogues: isozyme
773 selective inhibitors of protein kinase C beta. *J Med Chem* 39: 2664-2671
774 Kehoe DE, Jing D, Lock LT, Tzanakakis ES (2010) Scalable stirred-suspension bioreactor culture
775 of human pluripotent stem cells. *Tissue Eng Part A* 16: 405-421
776 Khan SA, Park KM, Fischer LA, Dong C, Lungjangwa T, Jimenez M, Casalena D, Chew B,
777 Dietmann S, Auld DS *et al* (2021) Probing the signaling requirements for naive human
778 pluripotency by high-throughput chemical screening. *Cell Rep* 35: 109233
779 Kim MH, Kino-Oka M (2020) Bioengineering Considerations for a Nurturing Way to Enhance
780 Scalable Expansion of Human Pluripotent Stem Cells. *Biotechnol J* 15: e1900314
781 Kim MH, Takeuchi K, Kino-Oka M (2019) Role of cell-secreted extracellular matrix formation in
782 aggregate formation and stability of human induced pluripotent stem cells in suspension culture. *J*
783 *Biosci Bioeng* 127: 372-380

784 Kinehara M, Kawamura S, Tateyama D, Suga M, Matsumura H, Mimura S, Hirayama N, Hirata
785 M, Uchio-Yamada K, Kohara A *et al* (2013) Protein kinase C regulates human pluripotent stem
786 cell self-renewal. *PLoS One* 8: e54122
787 Kitano Y, Nishimura S, Kato TM, Ueda A, Takigawa K, Umekage M, Nomura M, Kawakami A,
788 Ogawa H, Xu H *et al* (2022) Generation of hypoimmunogenic induced pluripotent stem cells by
789 CRISPR-Cas9 system and detailed evaluation for clinical application. *Mol Ther Methods Clin*
790 *Dev* 26: 15-25
791 Krawetz R, Taiani JT, Liu S, Meng G, Li X, Kallos MS, Rancourt DE (2010) Large-scale
792 expansion of pluripotent human embryonic stem cells in stirred-suspension bioreactors. *Tissue*
793 *Eng Part C Methods* 16: 573-582
794 Kwok CK, Ueda Y, Kadari A, Gunther K, Ergun S, Heron A, Schnitzler AC, Rook M, Edenhofer
795 F (2018) Scalable stirred suspension culture for the generation of billions of human induced
796 pluripotent stem cells using single-use bioreactors. *J Tissue Eng Regen Med* 12: e1076-e1087
797 Lam AT, Chen AK, Ting SQ, Reuveny S, Oh SK (2016) Integrated processes for expansion and
798 differentiation of human pluripotent stem cells in suspended microcarriers cultures. *Biochem*
799 *Biophys Res Commun* 473: 764-768
800 Nakanishi M, Kurisaki A, Hayashi Y, Warashina M, Ishiura S, Kusuda-Furue M, Asashima M
801 (2009) Directed induction of anterior and posterior primitive streak by Wnt from embryonic stem
802 cells cultured in a chemically defined serum-free medium. *FASEB J* 23: 114-122
803 Nath SC, Nagamori E, Horie M, Kino-Oka M (2017) Culture medium refinement by dialysis for
804 the expansion of human induced pluripotent stem cells in suspension culture. *Bioprocess Biosyst*
805 *Eng* 40: 123-131
806 Nishimura K, Sano M, Ohtaka M, Furuta B, Umemura Y, Nakajima Y, Ikehara Y, Kobayashi T,
807 Segawa H, Takayasu S *et al* (2011) Development of defective and persistent Sendai virus vector:
808 a unique gene delivery/expression system ideal for cell reprogramming. *J Biol Chem* 286: 4760-
809 4771
810 Oh SK, Chen AK, Mok Y, Chen X, Lim UM, Chin A, Choo AB, Reuveny S (2009) Long-term
811 microcarrier suspension cultures of human embryonic stem cells. *Stem Cell Res* 2: 219-230
812 Okita K, Matsumura Y, Sato Y, Okada A, Morizane A, Okamoto S, Hong H, Nakagawa M,
813 Tanabe K, Tezuka K *et al* (2011) A more efficient method to generate integration-free human iPS
814 cells. *Nat Methods* 8: 409-U452
815 Olmer R, Lange A, Selzer S, Kasper C, Haverich A, Martin U, Zweigerdt R (2012) Suspension
816 culture of human pluripotent stem cells in controlled, stirred bioreactors. *Tissue Eng Part C*
817 *Methods* 18: 772-784
818 Rajendran G, Dutta D, Hong J, Paul A, Saha B, Mahato B, Ray S, Home P, Ganguly A, Weiss
819 ML *et al* (2013) Inhibition of protein kinase C signaling maintains rat embryonic stem cell
820 pluripotency. *J Biol Chem* 288: 24351-24362

821 Ring DB, Johnson KW, Henriksen EJ, Nuss JM, Goff D, Kinnick TR, Ma ST, Reeder JW,
822 Samuels I, Slabiak T *et al* (2003) Selective glycogen synthase kinase 3 inhibitors potentiate
823 insulin activation of glucose transport and utilization in vitro and in vivo. *Diabetes* 52: 588-595
824 Rohani L, Borys BS, Razian G, Naghsh P, Liu S, Johnson AA, Machiraju P, Holland H, Lewis
825 IA, Groves RA *et al* (2020) Stirred suspension bioreactors maintain naive pluripotency of human
826 pluripotent stem cells. *Commun Biol* 3: 492
827 Shafa M, Sjonnesen K, Yamashita A, Liu S, Michalak M, Kallos MS, Rancourt DE (2012)
828 Expansion and long-term maintenance of induced pluripotent stem cells in stirred suspension
829 bioreactors. *J Tissue Eng Regen Med* 6: 462-472
830 Si-Tayeb K, Noto FK, Nagaoka M, Li J, Battle MA, Duris C, North PE, Dalton S, Duncan SA
831 (2010) Highly efficient generation of human hepatocyte-like cells from induced pluripotent stem
832 cells. *Hepatology* 51: 297-305
833 Singh H, Mok P, Balakrishnan T, Rahmat SN, Zweigerdt R (2010) Up-scaling single cell-
834 inoculated suspension culture of human embryonic stem cells. *Stem Cell Res* 4: 165-179
835 Steiner D, Khaner H, Cohen M, Even-Ram S, Gil Y, Itsykson P, Turetsky T, Idelson M,
836 Aizenman E, Ram R *et al* (2010) Derivation, propagation and controlled differentiation of human
837 embryonic stem cells in suspension. *Nat Biotechnol* 28: 361-364
838 Sumi T, Tsuneyoshi N, Nakatsuji N, Suemori H (2008) Defining early lineage specification of
839 human embryonic stem cells by the orchestrated balance of canonical Wnt/beta-catenin,
840 Activin/Nodal and BMP signaling. *Development* 135: 2969-2979
841 Takahashi K, Tanabe K, Ohnuki M, Narita M, Ichisaka T, Tomoda K, Yamanaka S (2007)
842 Induction of pluripotent stem cells from adult human fibroblasts by defined factors. *Cell* 131:
843 861-872
844 Takashima Y, Guo G, Loos R, Nichols J, Ficz G, Krueger F, Oxley D, Santos F, Clarke J,
845 Mansfield W *et al* (2014) Resetting transcription factor control circuitry toward ground-state
846 pluripotency in human. *Cell* 158: 1254-1269
847 Tannenbaum SE, Reubinoff BE (2022) Advances in hPSC expansion towards therapeutic entities:
848 A review. *Cell Prolif*: e13247
849 Toullec D, Pianetti P, Coste H, Bellevergue P, Grand-Perret T, Ajakane M, Baudet V, Boissin P,
850 Boursier E, Loriolle F *et al* (1991) The bisindolylmaleimide GF 109203X is a potent and
851 selective inhibitor of protein kinase C. *J Biol Chem* 266: 15771-15781
852 Tran TH, Wang X, Browne C, Zhang Y, Schinke M, Izumo S, Burcin M (2009) Wnt3a-induced
853 mesoderm formation and cardiomyogenesis in human embryonic stem cells. *Stem Cells* 27: 1869-
854 1878
855 Tsukamoto S, Nakade K, Wakabayashi T, Nakashima K, Takami M, Hemmi Y, Kuramochi Y,
856 Shimizu T, Arai Y, Matsuo-Takasaki M *et al* (2021) Generation of two ISL1-tdTomato reporter
857 human induced pluripotent stem cell lines using CRISPR-Cas9 genome editing. *Stem Cell Res* 53:
858 102363

859 Vijayaragavan K, Szabo E, Bosse M, Ramos-Mejia V, Moon RT, Bhatia M (2009) Noncanonical
860 Wnt signaling orchestrates early developmental events toward hematopoietic cell fate from
861 human embryonic stem cells. *Cell Stem Cell* 4: 248-262
862 Wang Y, Chou BK, Dowey S, He C, Gerecht S, Cheng L (2013) Scalable expansion of human
863 induced pluripotent stem cells in the defined xeno-free E8 medium under adherent and
864 suspension culture conditions. *Stem Cell Res* 11: 1103-1116
865 Woll PS, Morris JK, Painschab MS, Marcus RK, Kohn AD, Biechele TL, Moon RT, Kaufman
866 DS (2008) Wnt signaling promotes hematoendothelial cell development from human embryonic
867 stem cells. *Blood* 111: 122-131
868 Xu C, Inokuma MS, Denham J, Golds K, Kundu P, Gold JD, Carpenter MK (2001) Feeder-free
869 growth of undifferentiated human embryonic stem cells. *Nat Biotechnol* 19: 971-974
870 Yu J, Vodyanik MA, Smuga-Otto K, Antosiewicz-Bourget J, Frane JL, Tian S, Nie J, Jonsdottir
871 GA, Ruotti V, Stewart R *et al* (2007) Induced pluripotent stem cell lines derived from human
872 somatic cells. *Science* 318: 1917-1920
873 Zweigerdt R, Olmer R, Singh H, Haverich A, Martin U (2011) Scalable expansion of human
874 pluripotent stem cells in suspension culture. *Nat Protoc* 6: 689-700

875

Figures and Tables

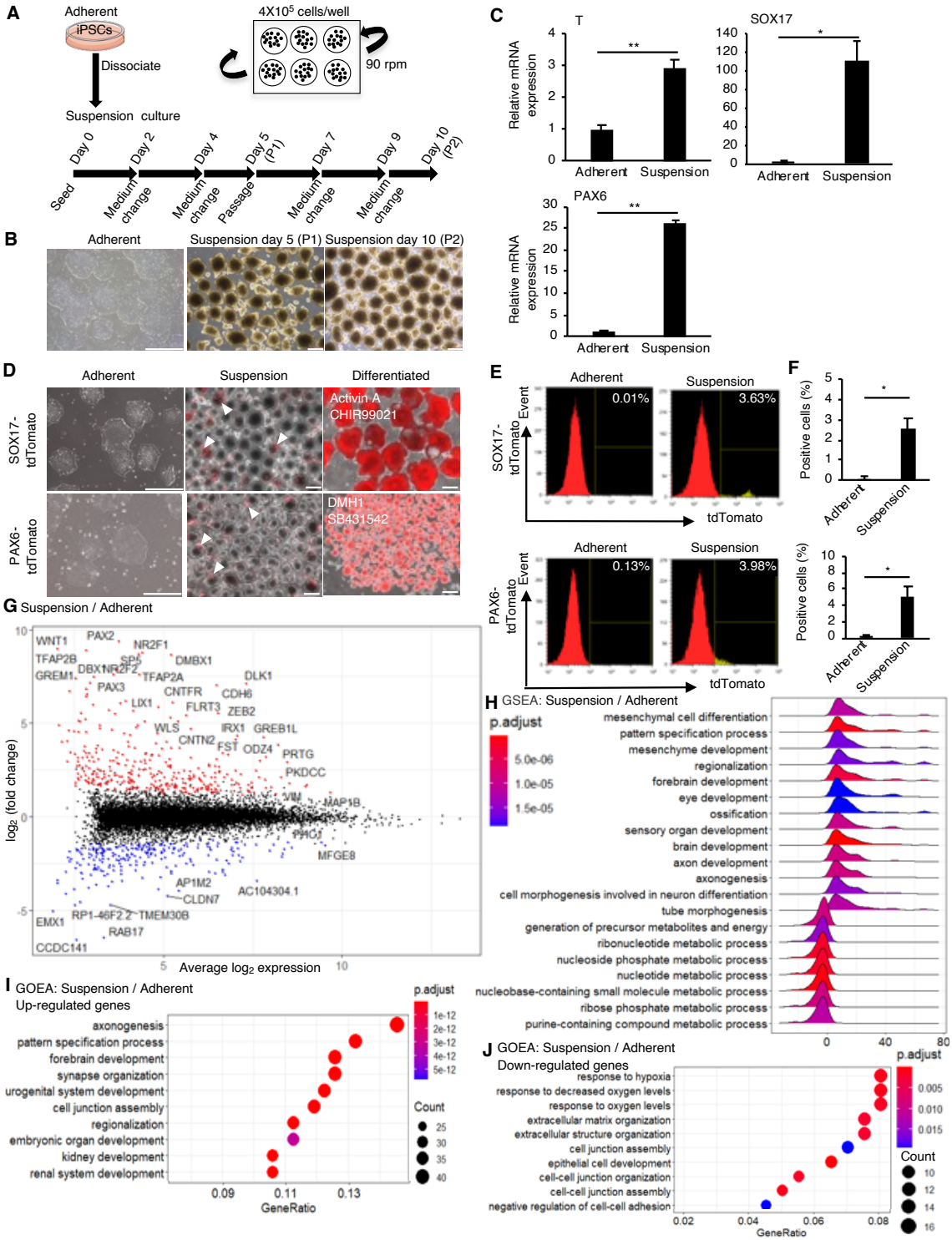

Figure. 1. HiPSCs maintained under suspension-culture conditions undergo spontaneous differentiation. (A) Schematics representing hiPSCs in suspension-culture conditions. (B) Phase-contrast images of adherent- or suspension-cultured hiPSCs on day 5 (Passage 1 (P1)) and day 10

881 (Passage 2 (P2)). Scale bars: 400 μm. (C) Gene expression in hiPSCs cultured under adherent or
882 suspension conditions on P2. Bar graphs show the mean ± SE (n=3). P-values were statistically
883 analyzed by Student's t-test. (D) Phase-contrast and fluorescent images of adherent or suspension-
884 cultured reporter hiPSCs on P2. White arrowheads indicate spontaneous expression of SOX17
885 and PAX6 in suspension conditions. Scale bars: 400 μm. (E) Quantification of hiPSCs
886 spontaneous differentiation with flow cytometry. (F) Averaged tdTomato-positive cell ratio (%)
887 from flow cytometry data (mean ± SE from n=3). P-values were statistically analyzed by
888 Student's t-test. (G) An MA plot comparing transcriptomes between suspension- and adherent-
889 culture from RNA-seq data. The representative gene name is shown in the plot. (H) GSEA on the
890 gene sets of suspension-cultured hiPSCs to adherent cultures. Adjusted P-values are shown as
891 blue to red from low to high values. (I and J) GOEA on the gene sets of suspension-cultured
892 hiPSCs to adherent culture. Results are ranked by significance (p-adjusted value) and/or counted
893 gene numbers.

894

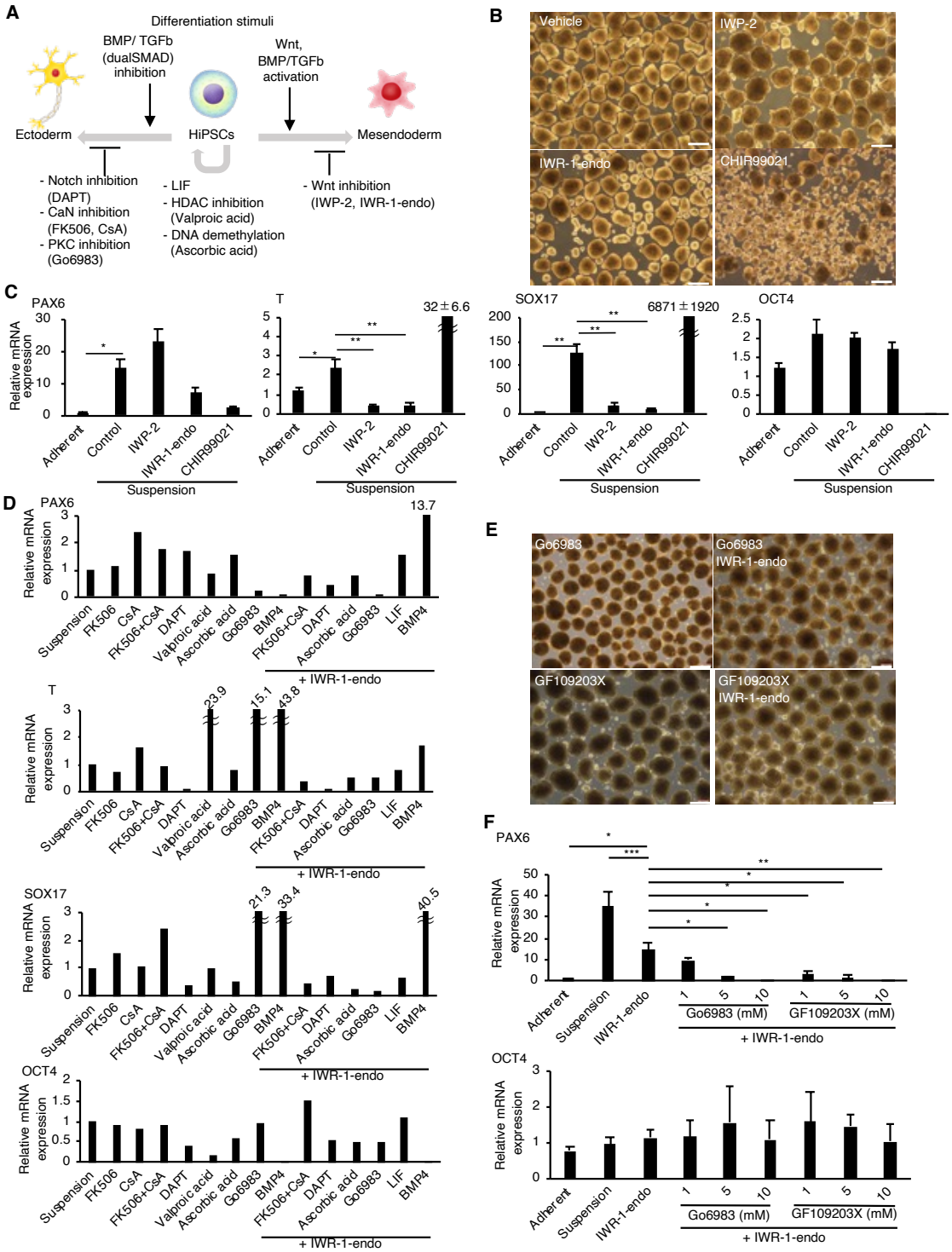

Figure 2. PKC inhibitors suppress spontaneous differentiation of hiPSCs into neural ectoderm in suspension-culture conditions. (A) Schematics. (B) Phase-contrast pictures of suspension-cultured hiPSCs in the presence of Wnt signaling inhibitors (IWP-2 and IWR-1-endo) or activator (CHIR99021). Scale bars: 400 μm. (C) Gene expression of hiPSCs in suspension-

899 culture conditions with or without IWP2, IWR-1-endo or CHIR99021. RT-qPCR was performed
900 on day 10 samples (P2). Gene expressions were normalized to GAPDH and displayed as relative
901 fold increase to adherent-cultured samples. Bar graphs show the mean ± SE. P-values were
902 statistically analyzed using Dunnett's multiple comparisons test. (D) Screening of inhibitory
903 activity of candidate molecules on neuroectoderm differentiation in suspension-cultured hiPSCs.
904 Candidate molecules were added in combination as shown. Results are displayed as relative fold
905 increase to suspension-cultured samples without pharmacological treatment. n=1. (E) Phase-
906 contrast images of suspension-cultured hiPSCs on P2 in the presence of PKC inhibitors (Go6983
907 or GF109203X) alone, or in combination with IWR-1-endo. Scale bars: 400 μm. (F) Suspension-
908 cultured hiPSCs gene expression in the presence of IWR-1-endo or with combined IWR-1-endo
909 and different doses of PKC inhibitors. Results are displayed as relative fold increase to adherent-
910 culture. Data are presented as mean ± SE (n=3).
911

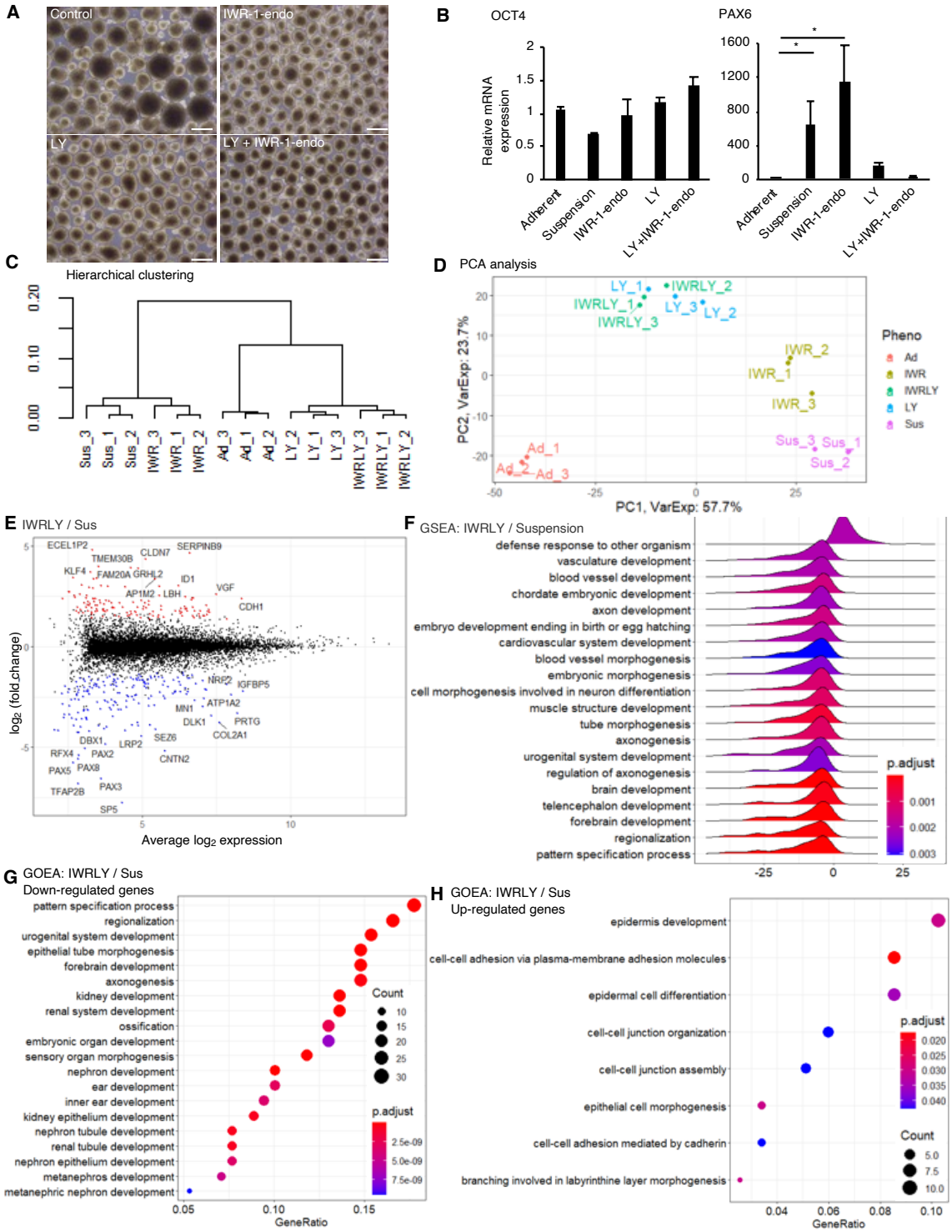

Figure 3. The inhibitors of WNT and PKCβ efficiently maintain the self-renewal of hiPSCs in suspension conditions. (A) Phase-contrast images of suspension-cultured hiPSCs on P2 in the presence of IWR-1-endo, LY333531, or both. Scale bars: 400 μm. (B) Gene expression of suspension-cultured hiPSCs on P2 in the presence of IWR-1-endo, LY333531, or both. Data are

916 presented as mean ± SE. P-values were statistically analyzed with Dunnett's test. (C) Hierarchical
917 clustering of adherent and suspension-cultured hiPSCs on P2 using Ward's method from RNA-
918 seq data (n=3 in each condition). Ad, Adherent; Sus, Suspension; IWR, IWR-1-endo; LY,
919 LY333531; IWRLY, IWR-1-endo and LY333531. (D) Principal component analysis (PCA) plot
920 showing clusters of samples based on similarity. Gene expression variance are displayed as PC1
921 and PC2. (E) MA plot comparing transcriptomes between IWRLY and Sus. (F) GSEA on the
922 gene sets of IWRLY to Sus from these RNA-seq data. Statistically significant enrichment is
923 shown. P-values are represented in blue to red from low to high values. (G and H) GOEA for the
924 gene sets of IWRLY to Sus from these RNA-seq data. Analysis was performed on down-
925 regulated genes in (G) and up-regulated genes in (H).
926

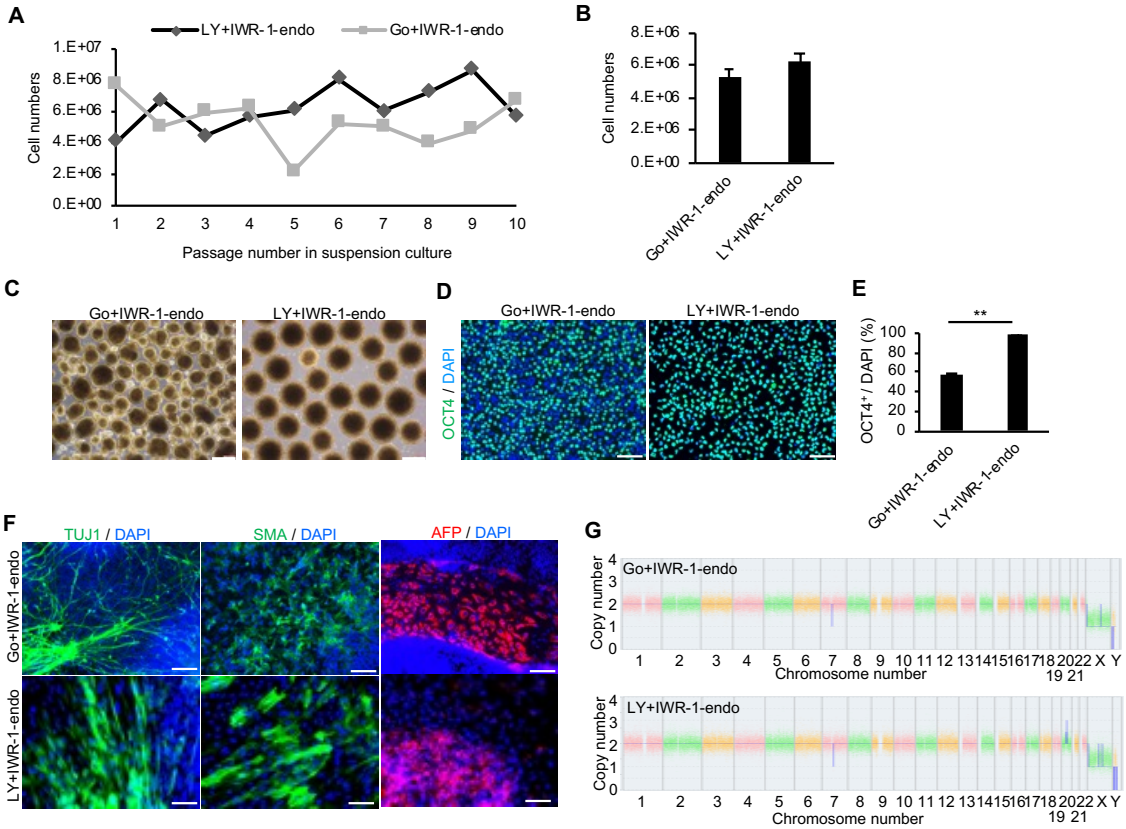

927 **Figure 4. Long-term suspension culture of hiPSCs is maintained by simultaneous**
928 **suppression of PKCβ and Wnt signals.** (A) The number of hiPSCs at passage during long-term
929 suspension-culture every 5 days. Cell culture was performed in the presence of IWR-1-endo plus
930 Go6983 or LY333531. (B) Bar graph indicating average cell numbers for 10 passages (mean ±
931 SE). (C) Phase-contrast images of suspension-cultured hiPSCs on passage 10. Scale bars: 400
932 μm. (D) Immunocytochemistry of OCT4 on passage 10 samples. Scale bars: 100 μm. (E) Bar
933 graph showing the percentages of OCT4 positive cells. Values were calculated from randomly
934 selected three regions from immunofluorescence images. Data are presented as mean ± SE. P-
935 value was statistically analyzed by Student's t-test. (F) Immunocytochemistry of differentiated
936 cells in EBs from suspension-cultured hiPSCs in the presence of IWR-1-endo; and Go6983 or
937 LY333531. Anti-TUJ1, -SMA and -AFP antibodies were used to detect ectoderm, mesoderm and
938 endoderm differentiation, respectively. Scale bars:100 μm. (G) Chromosomal copy numbers
939 detected with CGH array analysis (Karyostat assay) of suspension-cultured hiPSCs in the
940 presence of IWR-1-endo; and Go6983 (Upper panel) or LY333531 (Lower panel) at passage 10.
941

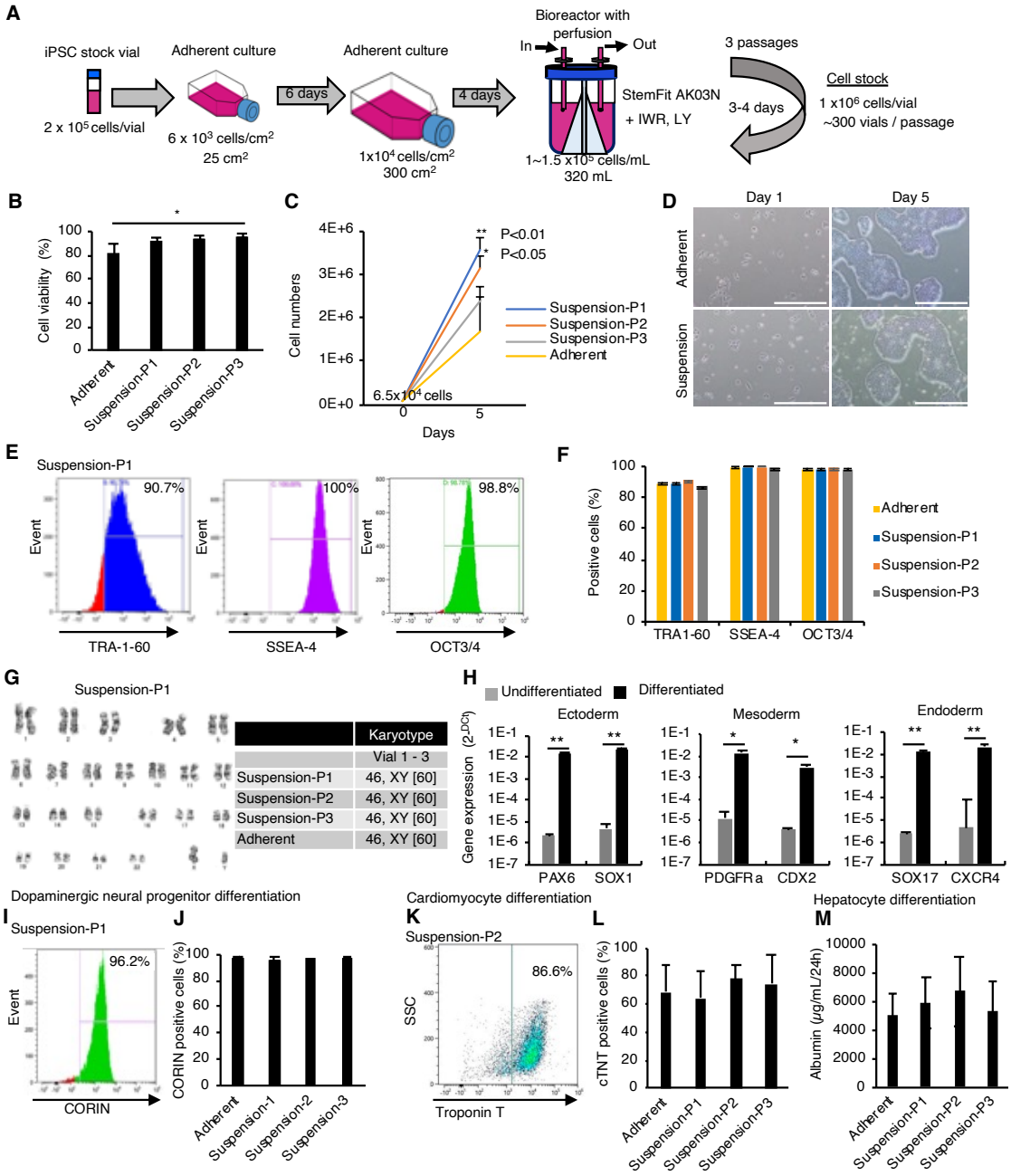

Figure 5. Mass suspension-culture of clinical-grade hiPSCs in the presence of PKCβ and Wnt signaling inhibitors. (A) Schematics. (B) Cell viability at seeding. Data are presented as mean ± SE (n=3). P-values were statistically analyzed with Dunnett's multiple comparisons test. (C) Total cell numbers were counted at day 5. Data were presented as mean ± SE (n=3). P-values were statistically analyzed with Dunnett's test. (D) Representative phase-contrast images of these hiPSCs. Scale bar: 1 mm. (E) Representative flow cytometry data of pluripotent markers in these hiPSCs. (F) Quantification of flow cytometry data for the pluripotent markers. Data are presented as mean ± SE (n=3). (G) Karyotypes of these hiPSCs. Left: Representative pictures of G-band

950 analysis. Right: Table of karyotype results (n=3). The numbers in brackets indicate the cell
951 numbers examined. (H) *In vitro* differentiation from hiPSCs was assessed using RT-qPCR (mean
952 ± SE) (n=3). P-value was statistically analyzed by Student's t-test. (I) Representative flow
953 cytometry data for CORIN. (J) Quantification of CORIN-positive cells (mean ± SE, n=3). (K)
954 Representative flow cytometry data for cardiac Troponin T (cTnT). (L) Quantification of cTnT-
955 positive cells (mean ± SE, n=3). (M) Albumin secretion levels of hepatocytes differentiated from
956 hiPSCs (mean ± SE, n=3).
957

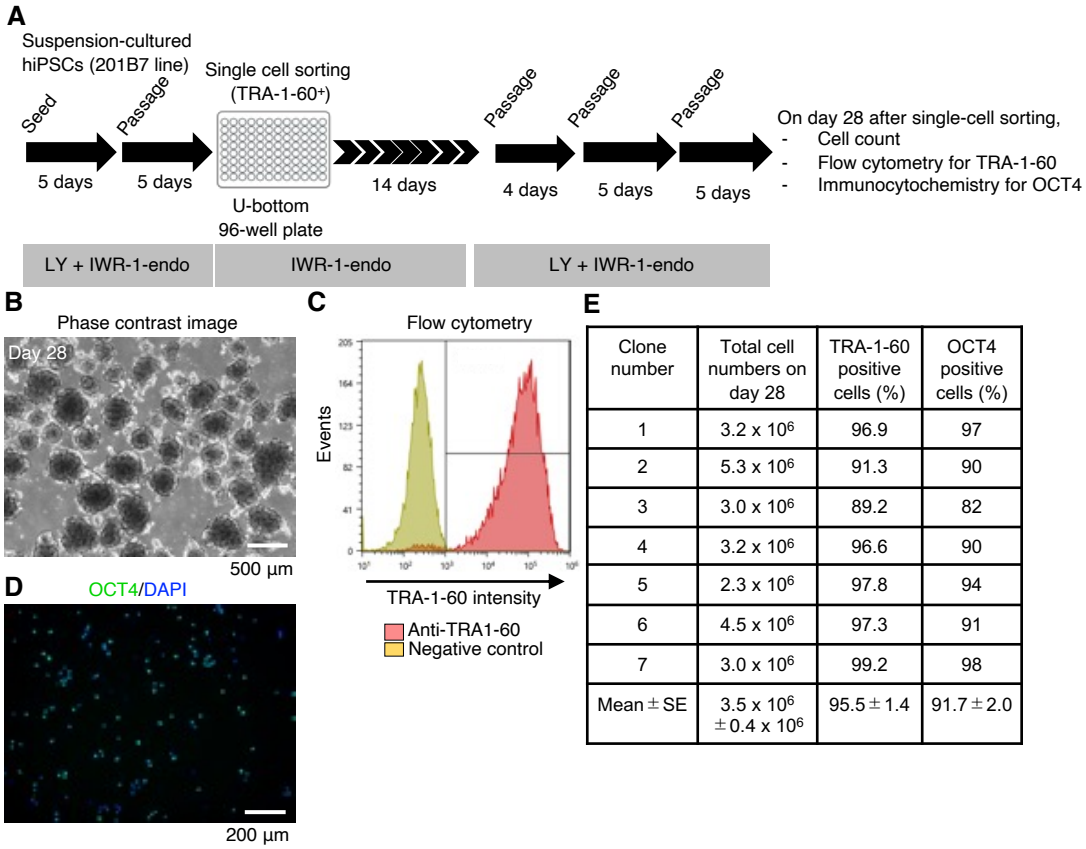

E

Clone number	Total cell numbers on day 28	TRA-1-60 positive cells (%)	OCT4 positive cells (%)
1	3.2×10^6	96.9	97
2	5.3×10^6	91.3	90
3	3.0×10^6	89.2	82
4	3.2×10^6	96.6	90
5	2.3×10^6	97.8	94
6	4.5×10^6	97.3	91
7	3.0×10^6	99.2	98
Mean ± SE	$3.5 \times 10^6 \pm 0.4 \times 10^6$	95.5 ± 1.4	91.7 ± 2.0

Figure 6. Establishment of single-cell-sorted hiPSC subclones cultured in suspension conditions supplemented with IWR1-endo and LY3333531. (A) Schematics representing the establishment of single-cell-derived hiPSC subclones from 201B7 line. Single-cell-sorted cells were expanded in the culture medium supplemented with IWR-1-endo and LY333531. Formed colonies were picked on day 14, and expanded by repeating passage every 4-5 days under suspension conditions. Characteristic analysis was performed on day 28 after single-cell-sorting. (B) Phase-contrast images of 201B7 on day 28 after single-cell sorting (Clone #2). Scale bars: 500 μm. (C) Represented flow cytometry of TRA-1-60 (Clone #2). (D) Represented immunocytochemistry of OCT4 (Clone #2). Scale bars: 200 μm. (E) Summary of the characterization of single cell-sorted clones. Total cell numbers on day 28, the ratio of TRA-1-60-positive cells (%), and the ratio of OCT4-positive cells (%) are shown (mean ± SE) (n=7).

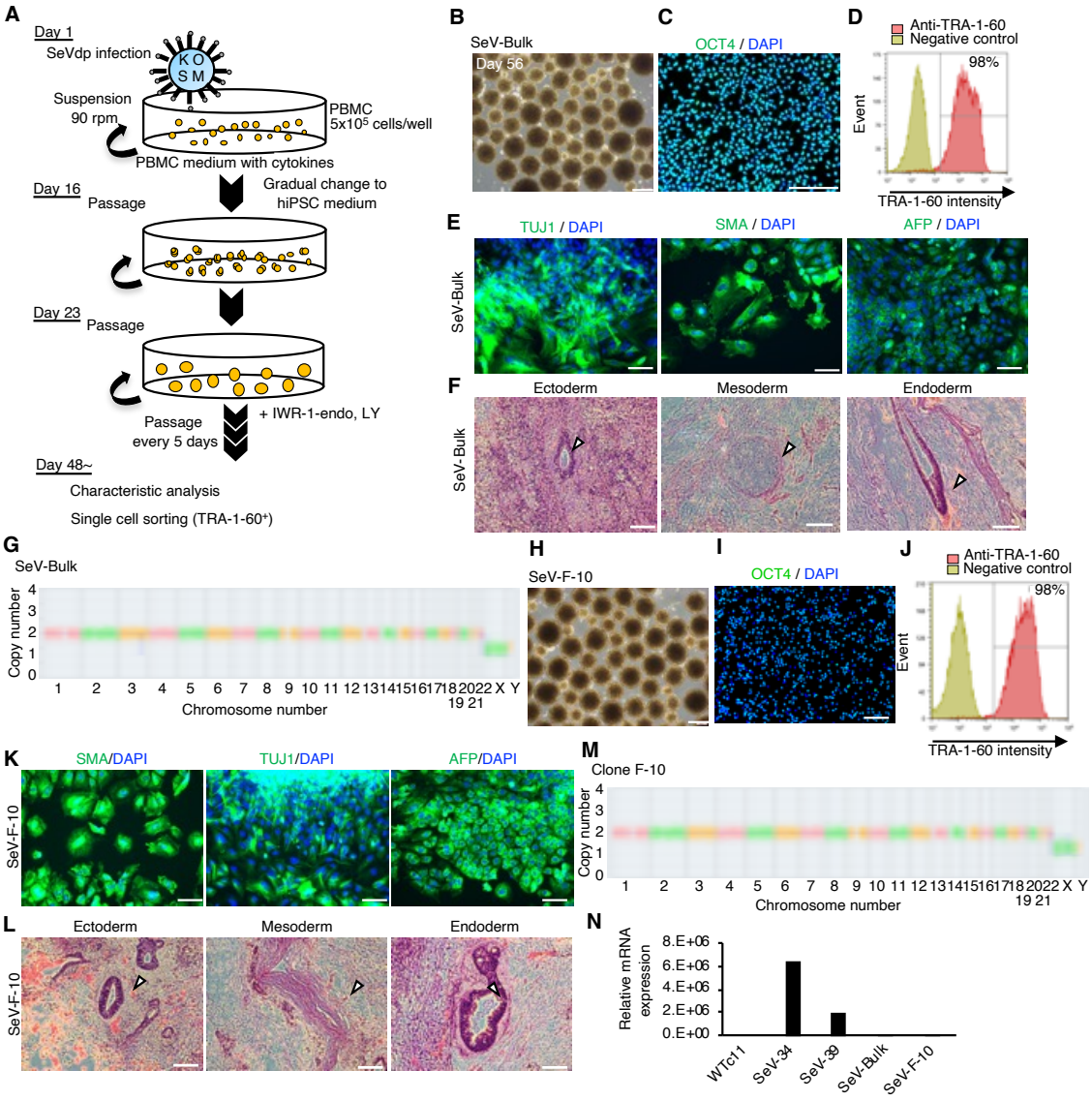

Figure 7. Establishment of hiPSCs in complete suspension conditions using SeVdp. (A) Schematics. (B) Phase-contrast images of PBMCs on day 56 after infection. Scale bars: 400 μm. (C) Immunocytochemistry of OCT4 on bulk-hiPSCs on day 56. Scale bars: 200 μm. (D) Flow cytometry of TRA-1-60 in bulk-hiPSCs on day 61. (E) Immunocytochemistry of TUJ1, SMA, and AFP on differentiated cells in EBs from bulk-hiPSCs on day 56. Scale bars: 100 μm. (F) HE staining of teratoma sections derived from bulk-hiPSCs. White arrowheads indicate representative tissue structures derived from ectoderm, mesoderm, and endoderm. Scale bars: 100 μm. (G) Chromosomal copy numbers detected with CGH array analysis on bulk-hiPSCs. (H) Phase-contrast image of an established hiPSC clone at passage 7. Scale bars: 400 μm. (I) Immunocytochemistry of established clone, F-10, with anti-OCT4 antibody. Scale bars: 200 μm.

980 (J) The percentage of TRA-1-60-positive cells with flow cytometry on established clone F-10
981 line. (K) HE staining of teratoma sections derived from F-10 clone line. The details are the same
982 as in (F). (L) Immunocytochemistry in EBs from established F-10 clone. Scale bars: 100 μm. (M)
983 Chromosomal copy numbers of F-10 clone line. (N) Residual SeVdp genomic RNA in
984 established hiPSCs with RT-qPCR.
985

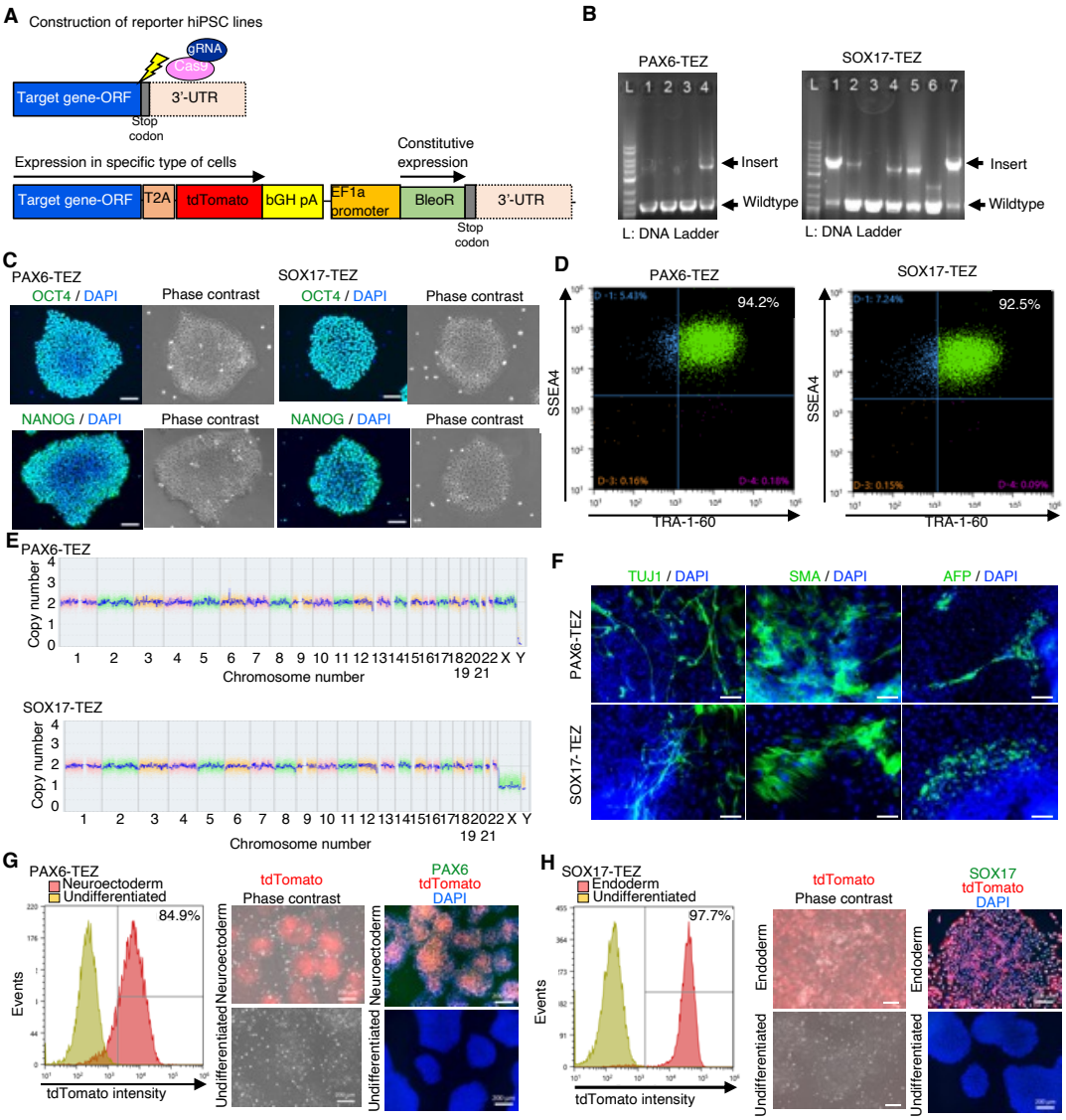

Figure 1–figure supplement 1. Characterization of PAX6-tdTomato and SOX17-tdTomato reporter lines. (**A**) Schematic of construction of reporter hiPSC lines. CRISPR/Cas9 was employed to knock-in the 2A-tdTomato gene and EF1a promoter-driven Zeocin (Bleomycin) resistance gene sequence (TEZ) to the 3' terminal of SOX17 or PAX6 open reading frame (ORF), respectively. (B) Genotyping of selected clones by genomic PCR. Arrows indicate alleles of wildtype or insertion in the PAX6 (left panel) or SOX17 (right panel) genes. (C) Phase-contrast images of representative colonies and immunocytochemistry of pluripotency markers: OCT4 and NANOG. Left panels: PAX6-TEZ. Right panels: SOX17-TEZ. (D) Flow cytometry of cell surface markers: TRA-1-60 and SSEA4. Left: PAX6-TEZ. Right: SOX17-TEZ. (E) Chromosomal copy numbers detected with CGH array analysis of PAX6-TEZ (top) and SOX17-

998 TEZ (bottom). (F) Immunocytochemistry of differentiated cells in EBs from established bulk-
999 hiPSCs on day 56. Anti-TUJ1, -SMA and -AFP antibodies were used. Scale bars: 100 μm. (G)
1000 Differentiation potency of PAX6-TEZ in the neural ectoderm. Left: Flow cytometry of tdTomato
1001 using PAX6-TEZ cultured in neuroectodermal differentiation medium for 7 days. Middle:
1002 Overlay images of phase-contrast and tdTomato fluorescence of PAX6-TEZ cultured in
1003 neuroectodermal differentiation medium (upper) or maintenance medium (lower). Right: Overlay
1004 images of tdTomato fluorescence and endogenous PAX6 protein detected with
1005 immunocytochemistry with anti-PAX6 antibody. (H) Differentiation potency of SOX17-TEZ in
1006 the endoderm. Left: Flow cytometry of tdTomato using SOX17-TEZ cultured in endodermal
1007 differentiation medium for 7 days. Middle: Overlay images of phase-contrast and tdTomato
1008 fluorescence of SOX17-TEZ cultured in endoderm differentiation medium (upper) or
1009 maintenance medium (lower). Right: Overlay images of tdTomato and endogenous SOX17
1010 protein detected by immunocytochemistry with anti-SOX17 antibody.
1011

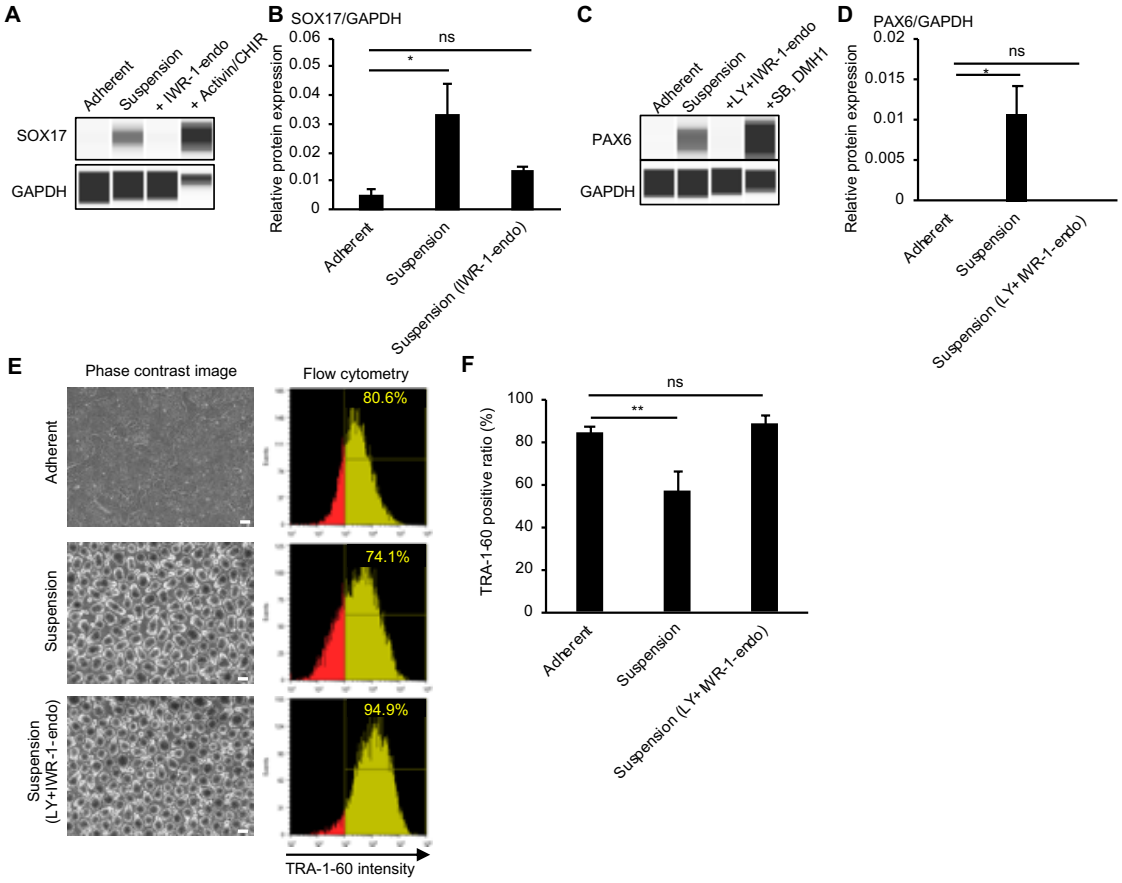

Figure 2−figure supplement 1. Effects of PKCβ and IWR-1-endo on suspension-cultured hiPSCs at the protein level. (A) Simple western blotting of adherent- or suspension-cultured hiPSCs (SOX17-TEZ) in the presence or absence of IWR-1-endo. SOX17-TEZ cultured in endoderm differentiation medium (Actinin A + CHIR) was used as a positive control for SOX17 expression. (B) Quantification of SOX17 expression. The protein expression was normalized to GAPDH. Data are presented as mean ± SE (n=3). (C) Simple western blotting of adherent- or suspension-cultured hiPSCs (PAX6-TEZ) in the presence or absence of IWR-1-endo and LY333531. PAX6-TEZ cultured in neurectoderm differentiation medium (SB431542+DMH1) was used as the positive control for PAX6 expression. (D) Quantification of expression of PAX6. The protein expression was normalized to GAPDH. Data are presented as mean ± SE (n=3). (E) Phase-contrast images and representative flow cytometry data of pluripotency marker, TRA-1-60, in adherent- or suspension-cultured hiPSCs (1383D6 line) on day10 (Passage 2). Suspension-culture was performed in the presence or absence of IWR-1-end and LY333531. The percentage of TRA-1-60 positive cells is shown in the right corner. (F) Quantified data for TRA-1-60 positive ratio (%). The percentage of TRA-1-60 positive cells is shown as mean ± SE (n=3).

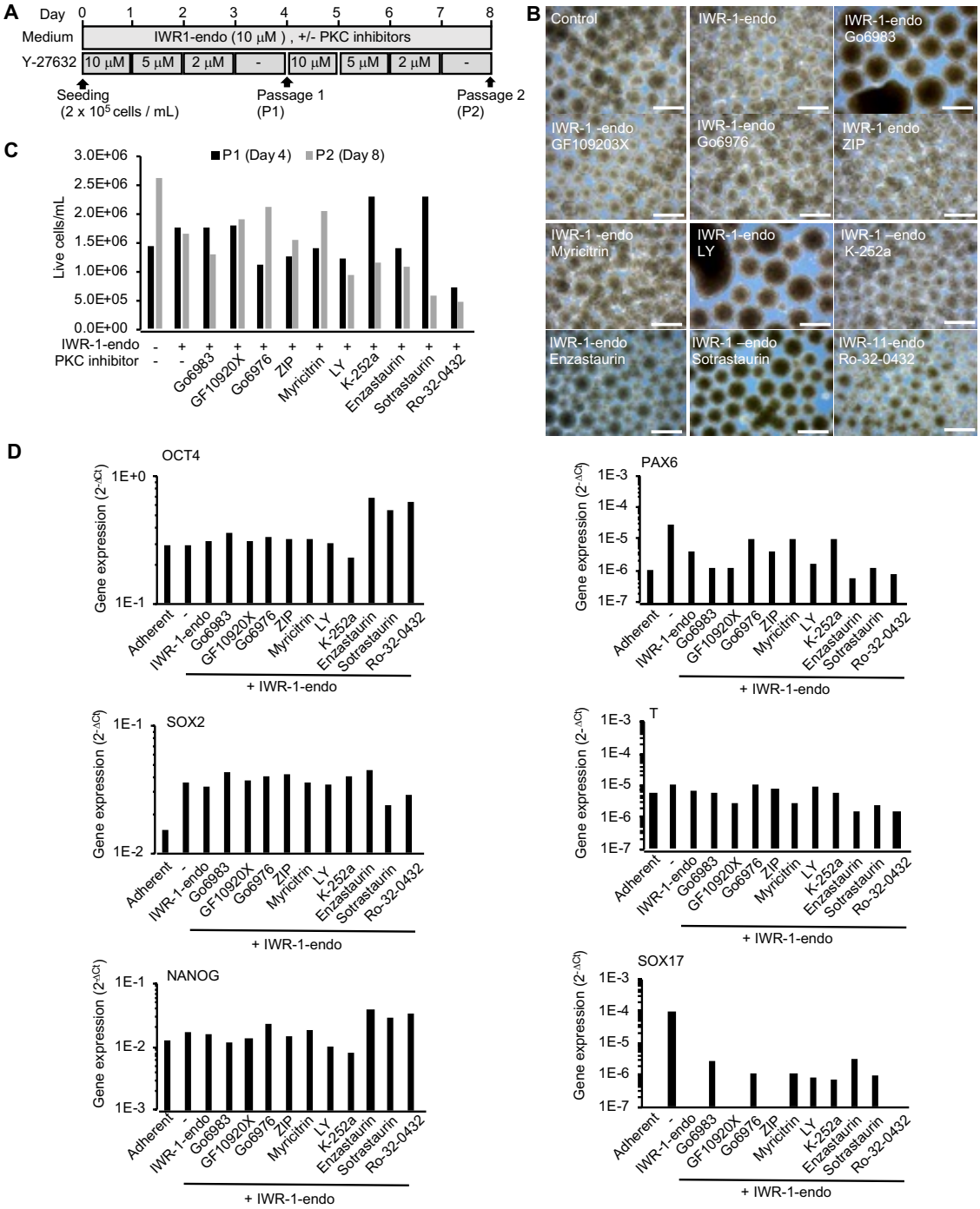

Figure 2–figure supplement 2. Activity of different type of PKC inhibitors on spontaneous differentiation of suspension-cultured hiPSCs. (A) Schematic representing suspension culture of hiPSCs supplemented with PKC inhibitors. Healthy donor-derived hiPSCs (201B7 line) were grown under continuous agitation in the presence of Y-27632, IWR-1-endo and PKC inhibitors. Passage was performed every four days. (B) Phase-contrast images of suspension cultured hiPSCs on day 8 (P2) in the absence or presence of IWR-1-endo and each PKC inhibitors. Scale

1034 bars, 500 μm. (C) Cell growth of hiPSCs (201B7). Graph shows live cell numbers counted on day
1035 4 and day 8 in suspension-culture (n=1). The PKC inhibitors added are labelled in the graphs. (D)
1036 Gene expression in hiPSCs cultured in adherent or suspension conditions with each PKC
1037 inhibitor. RT-qPCR was performed on cDNAs prepared from day 8 (passage 2) samples (n=1).
1038 qPCR was performed for pluripotency (OCT4, SOX2, NANOG) and early differentiation markers
1039 (PAX6, T, SOX17). Gene expression was normalized to beta-ACTIN.

1040

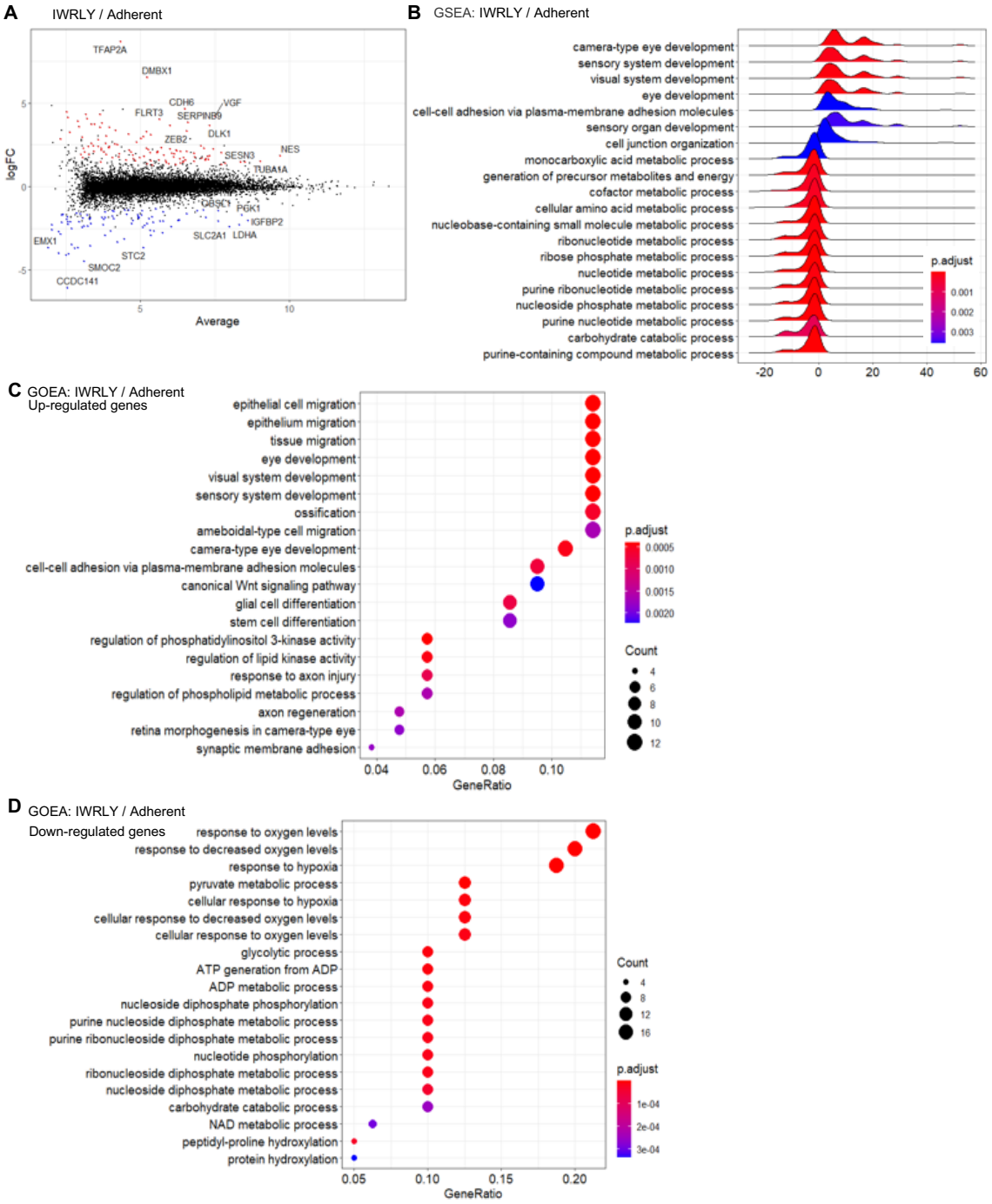

Figure 3–figure supplement 1. Global gene expression of suspension-cultured hiPSCs with IWR-1-endo and LY333531 in comparison to adherent-cultured hiPSCs. (A) MA plot (log2 fold change versus mean average expression) comparing the transcriptomes between adherent- and suspension-cultured hiPSCs treated with IWR-1-endo and LY33353 (IWRLY). Transcripts with log2 fold change ≧ 2 or ≦ -2 (FDR <0.01) are highlighted with red or blue dots,

1047 respectively. The names of the representative genes are shown in the plot. (B) GSEA of the gene
1048 sets of suspension-cultured hiPSCs with IWRLY compared to adherent-cultured hiPSCs.
1049 Analysis was performed on both up-regulated and down-regulated genes. Statistically significant
1050 enrichment is shown. Adjusted P-values are illustrated from blue to red as low to high. (C and D)
1051 GOEA of the gene sets of suspension-cultured hiPSCs with IWRLY compared to adherent-
1052 cultured hiPSCs. Analysis was performed on up-regulated genes in (C) and down-regulated genes
1053 in (D), respectively. Results are ranked by significance (adjusted P values) and/or counted gene
1054 numbers.
1055

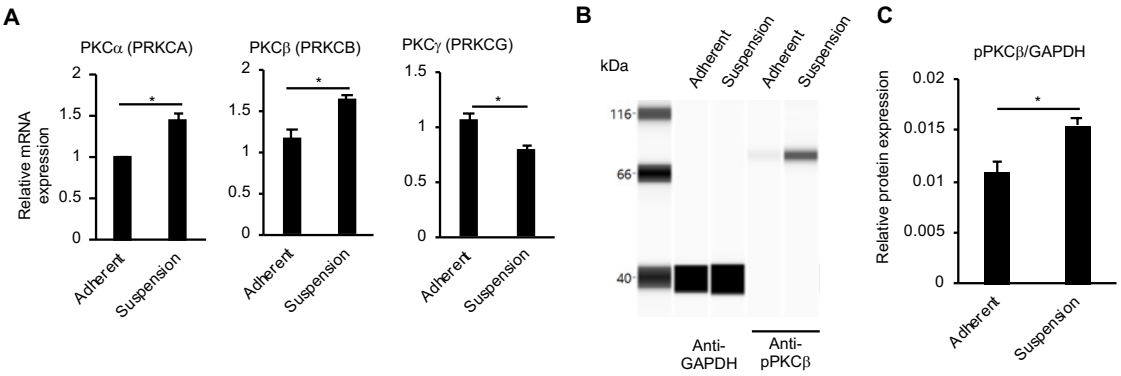

1056 **Figure 3—figure supplement 2. Up-regulation of PKC genes in suspension-cultured**
1057 **hiPSCs.** (A) RNA expression of conventional PKC isoform genes in hiPSCs as detected by RT-
1058 qPCR. cDNA was prepared from adherent- or suspension-cultured hiPSCs on day 5. The gene
1059 expression was normalized to GAPDH. Results are displayed as relative fold increase to
1060 adherent-culture. Data are presented as mean ± SE (n=3). P-values were statistically analyzed by
1061 Student's t-test. (B) Detection of phosphorylated PKCβ protein (pPKCβ) in suspension cultured
1062 hiPSCs on day 5 using an automated capillary western blot (Simple Western) assay. Adherent-
1063 cultured hiPSCs were used as a control. (C) Quantification of pPKCβ expression. The protein
1064 expression was normalized to GAPDH. Data are shown as mean ± SE (n=3). P-value was
1065 statistically analyzed using Student's t-test. Scale bars, 200 μm.
1066

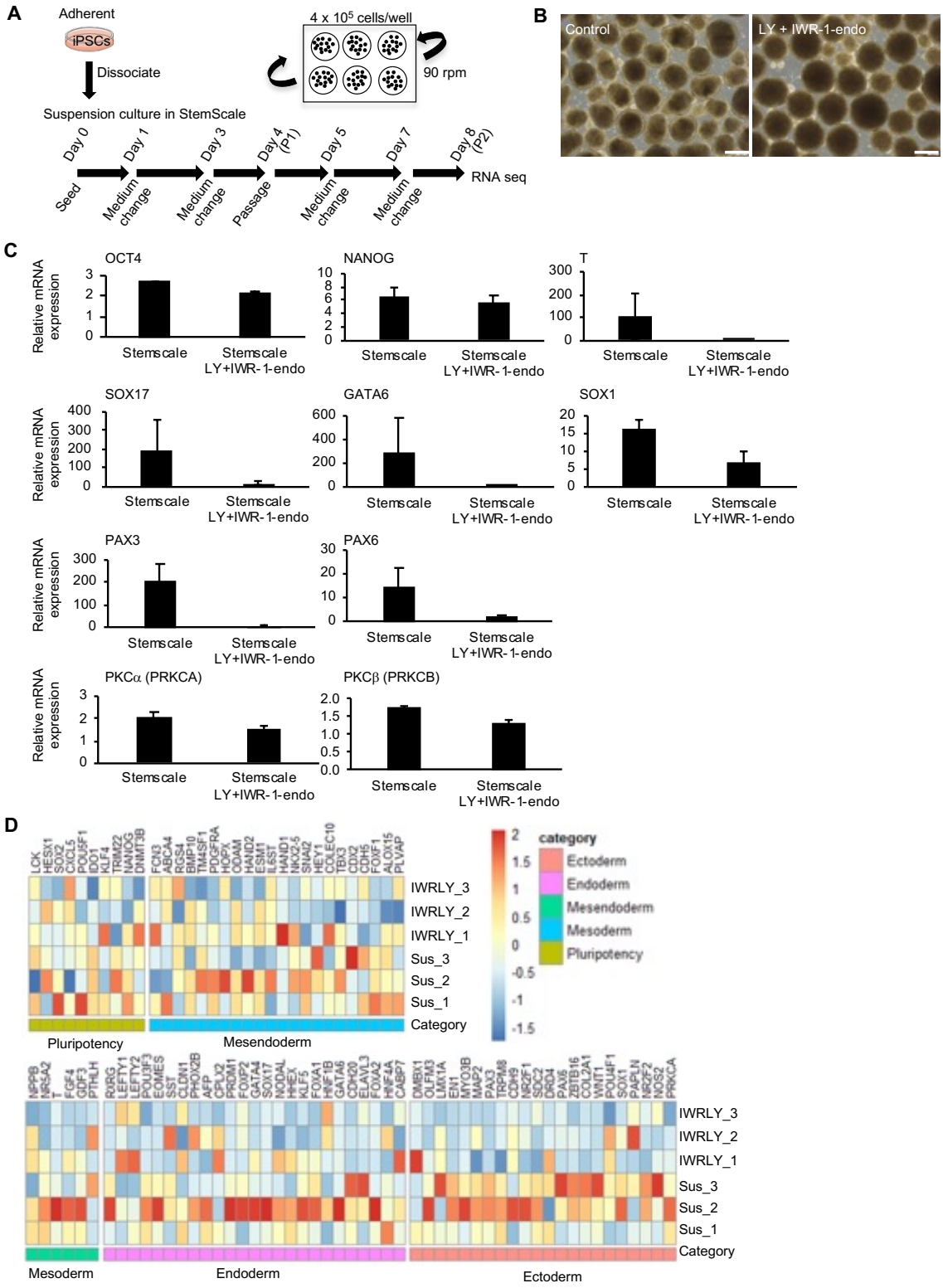

1067

1068 **Figure 4—figure supplement 1. Generality of the inhibitory effects of IWR-1-end and**

1069 **LY333531 on spontaneous differentiation of hiPSCs cultured in suspension condition.** (A)

1070 Schematic representing suspension culture of hiPSCs using StemScale medium (Thermo Fisher
1071 Scientific) as the basic culture medium. hiPSCs were grown under continuous agitation (90 rpm)
1072 in the presence or absence of IWR-1-endo and LY333531. Passage was performed every four
1073 days according to the manufacture's protocol. cDNAs were prepared from day 8 (P2) and used
1074 for RNA seq. (B) Phase-contrast images of suspension cultured hiPSCs on day 8 in the presence
1075 or absence of IWR-1-endo and LY333531. Scale bars, 400 μm. (C) RNA expression of
1076 pluripotency and early differentiated genes in hiPSCs, as detected by RT-qPCR. cDNA was
1077 prepared from suspension-cultured hiPSCs on day 8 in the presence or absence of IWR-1-endo
1078 and LY33353. The gene expression was normalized to GAPDH. Data are presented as mean ± SE
1079 (n=3). (D) Heat map of marker genes for pluripotency and differentiation to three germ layers
1080 from RNA-seq data in suspension-cultured iPSCs without compounds (Sus_1, Sus_2 and Sus_3)
1081 or with IWR-1-endo and LY333531 (IWRLY_1, IWRLY_2 and IWRLY_3). The listed genes
1082 were classified as pluripotent, mesendoderm, mesoderm, endoderm, and ectoderm, as defined in
1083 the Scorecard Assay (Thermo Fisher Scientific).
1084

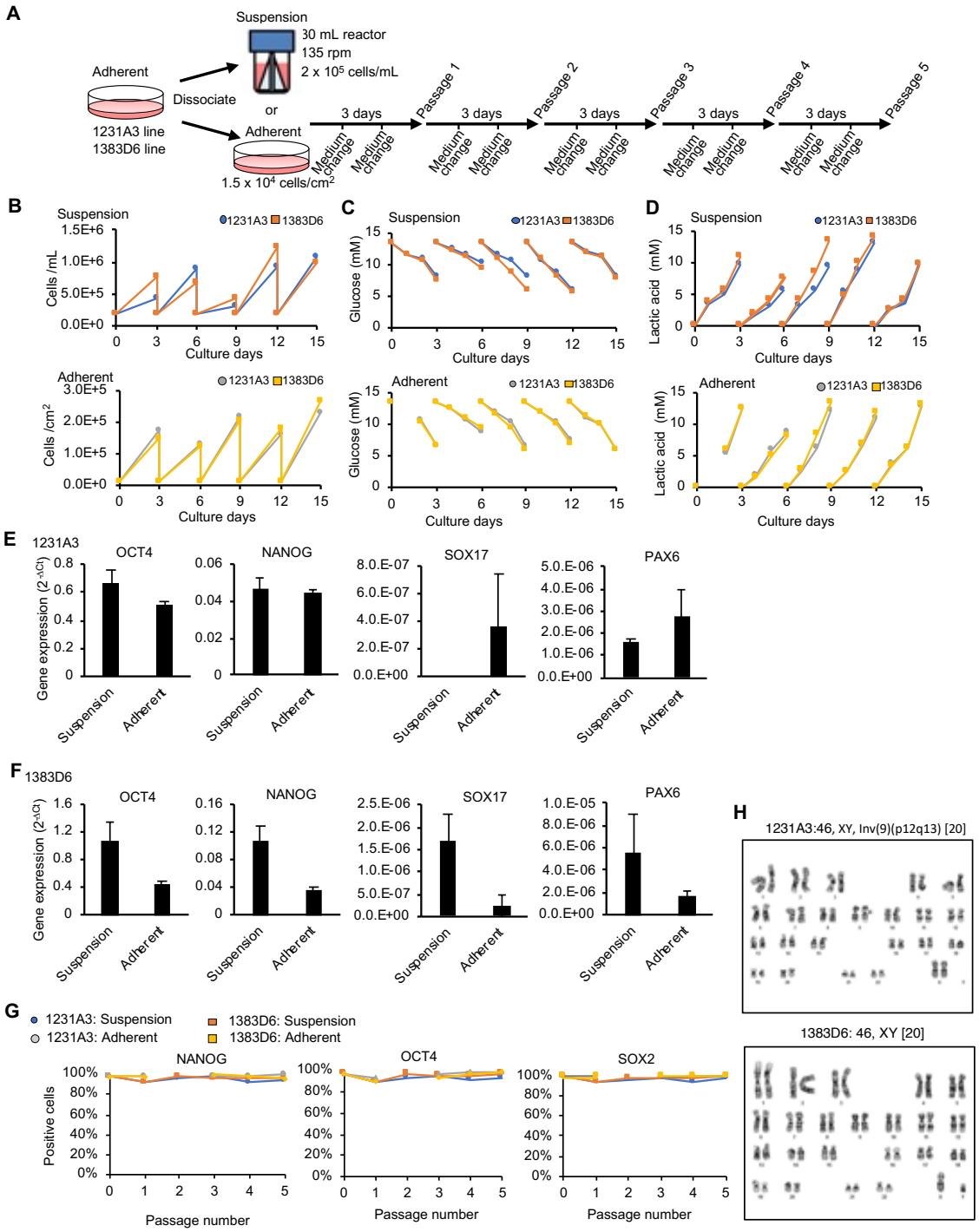

Figure 5–figure supplement 1. Suspension-culture of hiPSCs supplemented with IWR-1-endo and LY333531 using bioreactors with continuous agitation. (A) Schematic representing suspension culture of hiPSCs in a 30 mL bioreactor. Healthy donor-derived hiPSCs (1231A3 and 1383D6 lines) were grown with continuous agitation in the presence or absence of IWR-1-endo and LY333531. Passages were performed every three days. (B) Graphs showing cell numbers at

1091 each passage (n=1). Upper: suspension-culture of 1231A3 and 1383D6 lines. Lower: adherent-
1092 culture of 1231A3 and 1383D6 lines. (C) Graphs showing glucose concentration in the culture
1093 medium at each culture day. Upper: suspension-culture of 1231A3 and 1383D6 lines. Lower:
1094 adherent-culture of 1231A3 and 1383D6 lines. (D) Graphs showing lactic acid concentration in
1095 the culture medium at each culture day. Upper: suspension-culture of 1231A3 and 1383D6 lines.
1096 Lower: adherent-culture of 1231A3 and 1383D6 lines. (E and F) RT-qPCR analysis of hiPSCs
1097 cultured in 30 mL bioreactor or adherent conditions. cDNA samples were prepared from passage
1098 3 and 5 of the 1231A3 in (E) and 1383D6 in (F). qPCR was performed for *OCT4* and *NANOG*
1099 (pluripotent), *CDX2* (mesoderm), *SOX17* (endoderm) and *PAX6* (neuroectoderm). The gene
1100 expression was normalized to *β-ACTIN*. Bar graph showing the average gene expressions of
1101 passage 3 and 5 (mean ± SE). (G) Flow cytometric analysis of suspension- or adherent-cultured
1102 1231A3 and 1383D6 lines. Positive cells (%) of pluripotency marker proteins: NANOG, OCT4,
1103 and SOX2 are shown. (H) Karyotyping of hiPSCs cultured in 30 mL bioreactor. Cell samples
1104 were prepared on passage 5, and used for G-band karyotyping analysis. A short deletion on
1105 chromosome 9 of 1231A3 (indicated with arrow) was derived from the original line.

1106

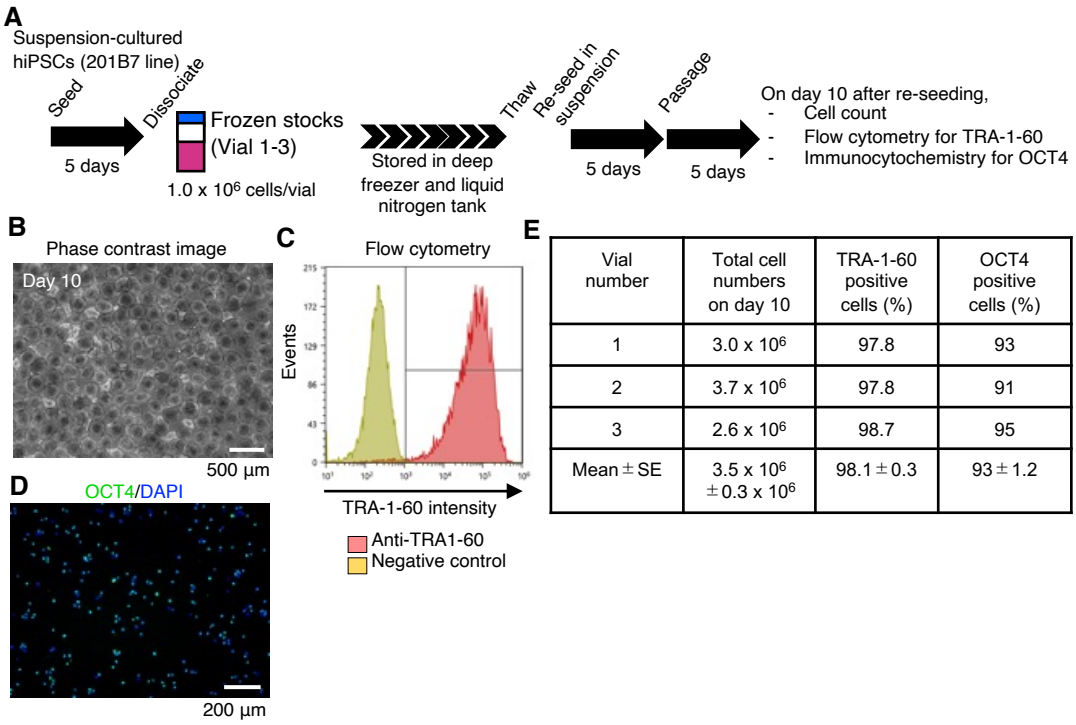

Vial number	Total cell numbers on day 10	TRA-1-60 positive cells (%)	OCT4 positive cells (%)
1	3.0×10^6	97.8	93
2	3.7×10^6	97.8	91
3	2.6×10^6	98.7	95
Mean ± SE	$3.5 \times 10^6 \pm 0.3 \times 10^6$	98.1 ± 0.3	93 ± 1.2

Figure 6–figure supplement 1. Re-suspension from frozen stocks of hiPSCs under suspension culture conditions supplemented with IWR-1-endo and LY333531. (A) Schematics of re-suspension culture of frozen stocks of single-cells-derived 201B7 clone (Vial 1-3). (B) Represented phase-contrast images on day 10 (Vial 3). Scale bars: 500 μm. (C) Represented flow cytometry of TRA-1-60 (Vial 3). (D) Represented immunocytochemistry of OCT4 (Vial 3). Scale bars: 200 μm. (E) Summary of the characterization of re-suspension-cultured iPSCs from frozen stocks. Total cell numbers on day 10, the ratio of TRA-1-60-positive cells (%), and the ratio of OCT4-positive cells (%) are shown (mean ± SE) (n=3).

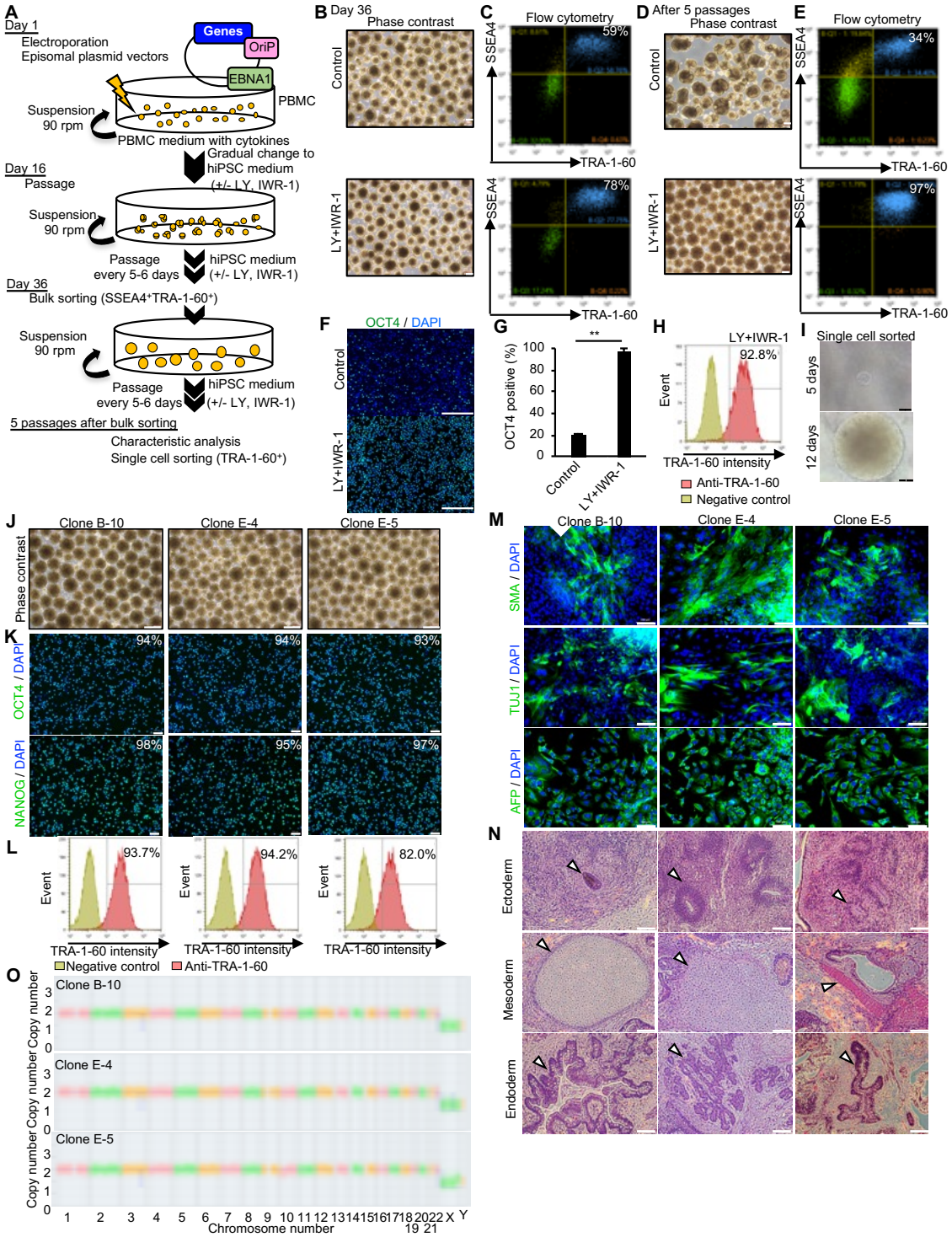

Figure 7–figure supplement 1. Establishment of hiPSCs in completed suspension conditions using episomal vectors. (A) Flow chart representing the establishment of hiPSCs from PBMCs by electroporation of episomal vectors. (B) Phase-contrast images of transfected cells on day 36 after electroporation of episomal vectors in the absence or presence of IWR-1-endo and

1122 LY333531. Scale bars: 400 μm. (C) Flow cytometry of TRA-1-60 and SSEA4. TRA-1-60 and
1123 SSEA4-psotive cells were sorted as the bulk fraction and further suspended in the absence or
1124 presence of IWR-1-endo and LY333531. The percentages of TRA-1-60 and SSEA4-psotive cells
1125 are shown in the right corner. (D) Phase-contrast images of suspension-cultured cell aggregates
1126 after bulk sorting on passage 5. Scale bars: 400 μm. (E) Flow cytometry of TRA-1-60 and
1127 SSEA4. The percentage of TRA-1-60- and SSEA4-psotive cells are shown in the right corner. (F)
1128 Immunocytochemistry of OCT4 on sorted-cells cultured in the absence (top) or presence (bottom)
1129 of IWR-1-endo and LY333531 for 5 passages. Scale bars: 400 μm. (G) Quantified data for
1130 OCT4-positive cell percentage. Bar graph indicating average OCT4-positive cell percentages
1131 (mean ± SE) (n=3). P-value was statistically analyzed by Student's t-test. (H) Single-cell sorting
1132 and cloning of TRA-1-60 positive cells. Flow cytometry was performed for cell fraction that was
1133 cultured in the presence of IWR-1-endo and LY333531. TRA1-60-positive cells were collected as
1134 single cells in a 96-well plate and expanded in the culture medium supplemented with Y-27632,
1135 IWR-1-endo and LY333531. (I) Representative phase-contrast images of single-sorted cell
1136 aggregates on day 5 and 12. Scale bars, 400 μm. (J) Phase-contrast images of established clones
1137 (B-10, E-4, and E-5). Scale bars: 400 μm. (K) Immunocytochemistry of OCT4 and NANOG in
1138 these clones. The percentage of positive cell are shown. Scale bars: 100 μm. (L) Flow cytometry
1139 of TRA-1-60 in these clones. TRA-1-60 positive percentages are shown in the right corner. (M)
1140 Immunocytochemistry of differentiated cells in EBs from these clones. Anti-TUJ1, -SMA and -
1141 AFP antibodies were used. Scale bars: 100 μm. (N) Hematoxylin-Eosin staining of paraffin-
1142 embedded sections of teratoma derived from these clones. White arrowheads indicate
1143 representative tissue structures of the ectoderm, mesoderm, or endoderm. Scale bars, 100 μm. (O)
1144 Chromosomal copy numbers detected by CGH array analysis (Karyostat assay) of these clones.

1145

1146 **Table 1. The list of published study on scalable suspension culture without microcarriers**
1147 **for hPSCs.**

Article	Medium	Additives	Cell lines tested	Scalability	Transcriptome	Single cell cloning	Direct freeze and thaw	iPSC generation
Matsuo-Takasaki et al. 2023 (This study)	AK02N, AK03N, StemScale	Y-27632, IWR-1-endo, LY333531	hiPSC (WTc11, 201B7, 1383D6, 1231A3, Ff-I14s04)	~10^9	Yes	Yes	Yes	Yes
Amit et al., 2010, 2011	DMEM/F12 + KSR	Y-27632, LIF, bFGF	hESC (I3, Ie, I5, H9.2, H9, H7, H14) hiPSC (iF4, J1.2.3, C3, C2, KTN7, KTN13)	~10^7	No	No	No	No
Krewetz et al., 2010	mTeSR1	Y-27632, Rapamycin	hESC (H9)	~10^8	No	No	No	No
Singh et al., 2010 Zweigerdt et al., 2011 Olmer et al., 2012	KnockOut DMEM + KSR, mTeSR1	Y-27632, bFGF	hESC (hES2, hES3, and ESI049) hiPSC (hCBiPS2, hiPSOCT4eGFP)	~10^8	No	No	No	No
Steiner et al., 2010	Neurobasal medium + KSR	Y-27632, bFGF, Activin A, Fibronectin, Gelatin, BDNF, NT3, NT4, Nutridoma-CS	hESC (HES1, HES2, H7)	~10^6	No	No	No	No (Of note, 3 hESC lines derivation)
Wang et al., 2013	TeSR-E8	Y-27632	hiPSC (BC1, TNC1)	~10^8	No	No	No	No
Hunt et al., 2014	mTeSR1	Y-27632	hESC (H1, H9)	~10^7	No	No	No	No
Elanzew et al., 2015	mTeSR1, TeSR-E8	Y-27632	hESC (H9) and hiPSC (iLB-C-31f-r1)	~10^7	No	No	No	No
Horiguchi et al., 2016; Ibuki et al., 2019	TeSR-E8, mTeSR1	Y-27632, KSR, Albumax, LPA, SIP,	hiPSC (TkDN4-M, TkDA3-4, 201B7)	~10^6	No	No	No	No
Nath et al., 2017	Dialyzed DMEM/F-12	Y-27632, bFGF, TGF-b1	hiPSC (Tic)	~10^8	No	No	No	No
Kwok et al, 2018	mTeSR1, StemMACS	Y-27632	hiPSC (AR1034ZIMA hiPSC clone1, FS hiPSC clone2)	~10^9	No	No	No	No
Rohani et al., 2020	mTeSR1, RSeT	Y-27632, Rapamycin	hESC (H1, H9)	~10^7	Yes	No	No	No

1148

1149 **Supplementary Table 1. The list of chemicals and cytokines used in the screening assay.**

Name	Effect	Manufacturer	Identifier	Concentration
CHIR99021	Wnt signal activator	Fujifilm Wako Pure Chemical	034-23103	3 μM
IWP-2	Wnt signaling inhibitor	Fujifilm Wako Pure Chemical	034-24301	5 μM
IWR-1-endo	Wnt signaling inhibitor	Fujifilm Wako Pure Chemical	037-25131	10 μM
Go6976	PKC (α, β) inhibitor	Fujifilm Wako Pure Chemical	071-06551	5 μM
Go6983	PKC (α, β, γ, δ) inhibitor	Fujifilm Wako Pure Chemical	078-06443	5 μM
GF109203X	PKC (α, β, γ) inhibitor	Tocris Bioscience	0741	5 μM
Enzastaurin	PKC (α, β, γ, ε) inhibitor	Sigma-Aldrich	SML0762	5 μM
K-252a	PKC (μ) inhibitor	Sigma-Aldrich	K1639	5 μM
LY333531 (Ruboxistaurin)	PKC (β) inhibitor	Sigma-Aldrich	SML0693	5 μM
Myricitrin	PKC (α, ε) inhibitor	Sigma-Aldrich	91255	5 μM
Sotrastaurin	PKC (α, β, δ, ε, η, θ) inhibitor	Cayman	16726	5 μM
ZIP	PKC (ζ) inhibitor	Tocris Bioscience	2549	5 μM
Ro-32-0432	PKC (α, β, γ, ε) inhibitor	Tocris Bioscience	1587	5 μM
FK506	Calcineurin inhibitor	Fujifilm Wako Pure Chemical	063-06071	100 ng/mL
Cyclosporine A (CsA)	Calcineurin inhibitor	Fujifilm Wako Pure Chemical	031-24931	1 mg/mL
DAPT	γ-secretase inhibitor	Fujifilm Wako Pure Chemical	043-33581	10 μM
BMP4 (Human, recombinant)	BMP-SMAD signaling activator	Fujifilm Wako Pure Chemical	020-18851	40 ng/mL
LIF (Human, recombinant)	LIF-STAT signaling activator	Nacalai Tesque	NU0013-1	2000 units/mL
Valproic acid (VPA)	Epigenetic modifier	Fujifilm Wako Pure Chemical	227-01071	0.5 mM
Ascorbic acid	Epigenetic modifier	Nacalai Tesque	13048-42	50 ng/mL

1150

1151 **Supplementary Table 2. The list of Taqman probes and primer sets used in this study.**

Target gene	Taqman Assay ID or sequence
ACTB	F: cctcatgaagatcctcaccga R: ttgccaatggtgatgacctgg
CDX2	F: cacccacagccatagacctac R: gtcagtccaggcaatgcttc
CXCR4	F: actgagaagcatgacggacaag R: aggtagcggtccagactgatg
GAPDH	Hs02786624_g1
GATA6	Hs00232018_m1
NANOG	Hs02387400_g1
OCT4 (POU5F1)	Hs04260367_gH
PAX3	Hs00240950_m1
PAX6	Hs01088114_m1
PDGFRa	F: gctgagcctaatcctctgcc R: actgctcacttccaagaccg
PKCα (PRKCA)	Hs00925200_m1
PKCβ (PRKCB)	Hs00176998_m1
PKCγ (PRKCG)	Hs00177010_m1
SOX1	Hs01057642_s1
SOX2	F: caccaatcccatccacactcac R: gcaaagctcctaccgtaccac
SOX17	Hs00751752_s1
T	Hs00610080_m1
SeV detection	F: accaacaggcggtggtgcaa R: tccaccccaacccctagcgt
PAX6 genotyping	F: ggaattccagtacttcacgtgaaggcatct R: tagaactgaagcggctctaacagccatttt
SOX17 genotyping	F: agaaaggggtgcctttagaggacgggtgtt R: aggaagtgtgtaacactgcttctggcctgc

1152

1153 **Supplementary Table 3. The list of primary antibodies used in this study.**

Name	Host species	Dilutions or Concentrations	SOURCE	IDENTIFIER
Alpha-Fetoprotein (AFP)	Mouse	1 μg/mL	R&D systems	Cat#MAB1368
Alpha-SMA	Mouse	1 μg/mL	R&D systems	Cat#MAB1420
Cardiac Troponin T	Mouse	10 μg/mL	Thermo Fisher Scientific	Cat#MA5-12960
CORIN	Mouse	10 μg/mL	Sigma-Aldrich	Cat#WH0010699M1
GAPDH	Mouse	1 μg/mL	R&D systems	Cat#MAB5718
NANOG	Rabbit	0.5 μg/mL	Reprocell	Cat#RCAB004P-F
OCT-3/4	Mouse	0.4 μg/mL	Santa Cruz	Cat#sc-5279
Oct-4A (C30A3) Rabbit mAb (Alexa Fluor 488 Conjugate)	Rabbit	1:30	Cell Signaling Technology	Cat# 5177S
PAX6	Rabbit	1:400 (Immunocytochemistry)	MBL	Cat#PD022
PAX6	Sheep	5 μg/mL (Wes)	R&D Systems	Cat#AF8150
Anti-PKC beta1 + PKC beta2 (phospho T641)	Rabbit	1:50	Abcam	Cat#ab194749
SOX17	Goat	0.4 μg/mL (Immunocytochemistry) 1 μg/mL (Wes)	R&D systems	Cat#AF1924
FITC Mouse anti-SSEA-4	Mouse	1:5	BD Bioscience	Cat#560126
APC anti-human SSEA4	Mouse	1:20	BioLegend	Cat#330418
Alexa Fluor 488 anti-human TRA1-60-R	Mouse	1:20	BioLegend	Cat#330614
Alexa Fluor 488 Mouse anti-Human TRA-1-60 Antigen	Mouse	1:10	BD Bioscience	Cat#560173
TUJ1	Mouse	1 μg/mL	R&D systems	Cat#MAB1195

1154 **Supplementary Table 4. The list of secondary antibodies used in this study.**

Name	Host species	Dilutions	SOURCE	IDENTIFIER
Anti-Mouse IgG (H+L) Highly Cross-Adsorbed Secondary Antibody, Alexa Fluor Plus 488	Donkey	1:1000	Thermo Fisher Scientific	Cat#A-21202
DyLight 488 anti-rabbit IgG (minimal x-reactivity)	Donkey	1:1000	BioLegend	Cat#406404
Anti-Mouse IgG (H+L) Highly Cross-Adsorbed Secondary Antibody, Alexa Fluor Plus 555	Donkey	1:1000	Thermo Fisher Scientific	Cat#A-31570
Anti-Rabbit IgG (H+L) Cross-Adsorbed Secondary Antibody, Alexa Fluor 555	Goat	1:1000	Thermo Fisher Scientific	Cat#A-21428
Anti-Mouse IgG (H+L) Cross-Adsorbed Secondary Antibody, Alexa Fluor 488	Goat	1:1000	Thermo Fisher Scientific	Cat#A-11001
Donkey Anti-Sheep IgG HRP Affinity Purified PAb	Sheep	1:50	R&D systems	Cat# HAF016

1155

1156 **Supplementary Table 5. Software used in this study.**
1157

Name	Source	URL
clusterProfiler (v3.16.1)	R package	https://bioconductor.org/packages/release/bioc/html/clusterProfiler.html
edgeR (v3.30.3)	R package	https://bioconductor.org/packages/release/bioc/html/edgeR.html
R (version4.1.0)	R package	https://www.r-project.org/
CLC Genomics Workbench (v20)	QIAGEN	https://digitalinsights.qiagen.com/products-overview/discovery-insights-portfolio/analysis-and-visualization/qiagen-clc-genomics-workbench/
Cell Sorter software	Sony	https://www.sonybiotechnology.com/us/instruments/sh800s-cell-sorter/software/
Compass software for Simple Western	Protein Simple	https://www.bio-techne.com/resources/instrument-software-download-center/compass-software-simple-western
BZ-X800 microscope analysis software	Keyence	https://www.keyence.com/landing/microscope/lp_fluorescence.jsp
QuantStudio 3 and 5 Real-Time PCR System Software	Thermo Fisher Scientific	https://www.thermofisher.com/jp/ja/home/global/forms/life-science/quantstudio-3-5-software.html
Chromosome Analysis Suite (ChAS) and Affymetrix GeneChip Command Console software programs	Thermo Fisher Scientific	https://www.thermofisher.com/jp/ja/home/life-science/microarray-analysis/microarray-analysis-instruments-software-services/microarray-analysis-software/chromosome-analysis-suite.html
CellSens microscope software	Evident (Olympus)	https://www.olympus-lifescience.com/en/support/downloads/

1158